# Spectroscopy and Structure of the Lithium Hydride Diatomic Molecules and Ions

**William C. Stwalley**

*Center for Laser Science and Engineering, and Departments of Chemistry, and of Physics and Astronomy, University of Iowa, Iowa City, IA 52242*

**and**

**Warren T. Zemke**

*Department of Chemistry, Wartburg College, Waverly, IA 50677*

Received August 10, 1992; revised manuscript received October 19,1992

All significant experimental measurements and many theoretical calculations of the spectroscopy and structure of the isotopic lithium hydrides ($^6$LiH, $^7$LiH, $^6$LiD, $^7$LiD) are identified and reviewed. Published molecular constant determinations from conventional and laser spectroscopy are evaluated; recommended spectroscopic constants for the $X\ ^1\Sigma^+$, $A\ ^1\Sigma^+$ and $B\ ^1\Pi$ states are tabulated. Potential energy curves (RKR, IPA and hybrid) for the $X\ ^1\Sigma^+$, $A\ ^1\Sigma^+$ and $B\ ^1\Pi$ states are evaluated and recommended curves are tabulated. Dissociation energy estimates are evaluated and recommended $D_0$ and $D_e$ values tabulated for the $X\ ^1\Sigma^+$, $A\ ^1\Sigma^+$ and $B\ ^1\Pi$ states. Accurate electronic structure calculations (Hartree Fock or better) on this "workbench of theoretical chemistry" are listed and described briefly; all excited electronic states considered are included. Experimental and theoretical radiative and dipole properties are noted and discussed. Adiabatic corrections to the Born-Oppenheimer approximation are also reviewed. Calculations on $LiH^+$ and $LiH^-$ are also listed and described briefly.

Key words: alkali hydride; Born-Oppenheimer approximation; dissociation energy; electronic structure calculation; isotope effects; LiH, $LiH^+$, $LiH^-$; potential energy curve; spectroscopic constant.

## Contents





### List of Tables

### List of Figures



## 1. Introduction

### 1.1. Introduction

Lithium hydride, the simplest neutral heteropolar diatomic molecule, has been the object of intense theoretical and spectroscopic study since the 1930's. The common isotopomers $^7$LiH, $^7$LiD, $^6$LiH and $^6$LiD have significantly different reduced masses (see Table 1). Many of the constants taken directly from the literature used the earlier isotopic masses from Wapstra and Bos [WAP 77]. The differences between the earlier [WAP 77] and current [WAP 85] masses are $<2\times10^{-8}$ amu for the hydrogen isotopes and $<2\times10^{-6}$ amu for the lithium isotopes. This should not affect the numbers reported here, except those given in Sec. 5 (which are based on [WAP 85]).

The lithium hydride system provides a number of different studies in addition to those reported for the other alkali hydrides [STW 91]: (i) detailed examination of the concept of mass-reduced quantum numbers, (ii) unique analyses of adiabatic and nonadiabatic breakdown of the Born-Oppenheimer approximation, and (iii) significant studies on the breakdown of the semiclassical approximation in the Rydberg-Klein-Rees (RKR) method of potential inversion, particularly near the dissociation limit and with a very weakly bound state.

TABLE 1. Atomic and reduced masses for lithium hydride[a]

| Isotope | Mass (amu)[b] | Isotopmer | μ(amu)[b] |
|---|---|---|---|
| $^7$Li | 7.0160030 | $^7$LiH | 0.88123816 |
| $^6$Li | 6.0151214 | $^7$LiD | 1.56487045 |
| $^1$H | 1.007825035 | $^7$LiT | 2.10930029 |
| $^2$H(≡D) | 2.014101779 | $^6$LiH | 0.86319752 |
| $^3$H(≡T) | 3.01604927 | $^6$LiD | 1.50887159 |
| | | $^6$LiT | 2.00880962 |

[a]Atomic isotopic masses are from Wapstra and Audi [WAP 85].
[b]1 atomic mass unit = $M(^{12}C)/12$.

Because of an ionic-covalent avoided crossing between the ground $X\,^1\Sigma^+$ state and the first excited $A\,^1\Sigma^+$ state potential energy curves, the behavior of the $A$ state is quite anomalous. According to Mulliken [MUL 36], the $X$ state has mostly $Li^+H^-$ character near its equilibrium internuclear distance $R_e$, while the $A$ state is predominantly $Li^+H^-$ in character at large $R$. Thus the $A$ state potential curve is flat bottomed (see Fig. 1) and highly anharmonic: the anharmonicity constant $\omega_e x_e$ is negative and the vibrational energy levels initially are more rather than less widely separated with increasing vibrational quantum number $v$. Although the anomalous behavior of the $A$ state is common to all the alkali hydrides [STW 91], LiH is of special interest for studying this behavior experimentally and theoretically.

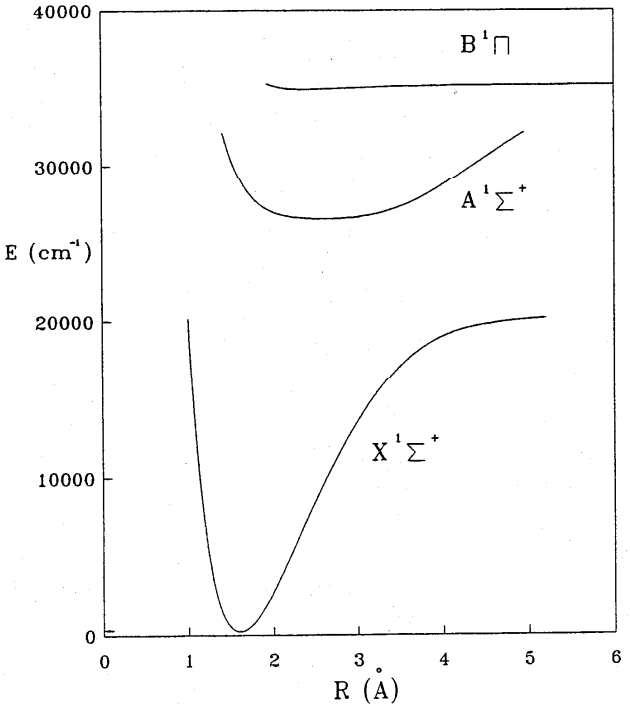


FIG. 1. Observed potential curves of LiH.

Of all the alkali hydrides, only in lithium hydride is the very shallow $B\ ^1\Pi$ state (see Fig. 1) well characterized experimentally. In the other alkali hydrides the $B$ state is determined theoretically, at various levels of approximation [STW 91]. One additional point about the $B$ state needs to be mentioned. The angular momentum quantum number $\Lambda = 1$ and a number of problems arise in the analysis of the $B$ state, distinct from the analyses of the $^1\Sigma^+$ states; in the $B$ state there are no $J = 0$ levels and the determination of $B$ state $D_e$ and $T_e$ values must take this into account.

Table 2 contains the recommended molecular structure constants for all observed isotopic combinations of the lithium hydrides and deuterides. All zero point energies are determined directly from adiabatically corrected spectroscopic constants (identified later in the text). In particular, the $D_e$, $D_0$ and $T_e$ values are discussed in Secs. 2.5, 2.5, and 2.3, respectively. $R_e$ values are determined from $B_e$ values in Sec. 2.4 (see also discussion in Sec. 3). Although molecular constants for the tritides are not reported per se in the literature, they can be accurately computed. Extrapolations to infinite nuclear mass (i.e. fixed nuclei) can be carried out for optimal comparison with fixed nuclei *ab initio* calculations.

For the hydride and deuteride data in Table 3, the following relations can be determined

$$D_e^X(M_H) = (20299.3 - 11.70/M_H)\ \text{cm}^{-1}$$
$$D_e^A(M_H) = (8687.7 - 6.25/M_H)\ \text{cm}^{-1}$$
$$D_e^B(M_H) = (293.2 - 4.44/M_H)\ \text{cm}^{-1}$$
$$T_e^A(M_H) = (26515.3 - 5.55/M_H)\ \text{cm}^{-1}$$
$$T_e^B(M_H) = (34909.8 - 7.36/M_H)\ \text{cm}^{-1}$$

where $M_H$ is the mass of the hydrogen isotope ($^1$H, $^2$H or $^3$H) in amu. The first number represents the $D_e$ or $T_e$ value for infinitely massive hydrogen nuclei. The corrections due to the Li mass are expected to be small for $D_e$ and known to be small for $T_e$ ($\lesssim 0.1\ \text{cm}^{-1}$).

Because of its simple electronic structure, LiH (along with $LiH^+$ and $LiH^-$) has been one of the theoreticians' favorite model systems for studying a variety of quantum mechanical techniques and approximations. Over 20 years ago, lithium hydride was called "the workbench of the theoretical chemist" [BEN 68]. The current literature is still filled annually with a long list of theoretical lithium hydride calculations of varying utility and complexity. There is no attempt here to identify literature references for each of the theoretical calculations on LiH and its ions. Rather, we consider only high quality calculations at the Hartree-Fock level or better; identified are calculations of electronic structure as well as other radiative, electric and magnetic properties. In addition, for earlier *ab initio* methods and calculated properties, we note a number of early compendia on LiH [CAD 67, KRA 67, RIC 71, RIC 74, RIC 78, RIC 81], $LiH^+$ [CAD 67, RIC 71, RIC 74, RIC 78, RIC 81] and $LiH^-$ [RIC 78, RIC 81].

Shorthand notations used to describe *ab initio* calculations will be given in the glossary. Common energy units used are $\text{cm}^{-1}$ and hartrees: 1 a.u. = 1 hartree = 219474.631418 $\text{cm}^{-1}$ [BIR 89], 1 eV = 8065.5438 $\text{cm}^{-1}$ [COH 90]. More complete lists may be found in the list of 1987 CODATA fundamental constants in [COH 87]. All reduced masses are based on the mass of carbon-12 $M(^{12}\text{C})$ equaling exactly 12. Distance units used are Å and $a_0$: 1 $a_0$ = 0.529177249 Å.

TABLE 2. Recommended molecular constants for lithium hydrides and deuterides

| Isotopomer | $D_e$ ($\text{cm}^{-1}$) | $D_0$ ($\text{cm}^{-1}$) | $R_e$ (Å) | $T_e$ ($\text{cm}^{-1}$) | Ref.[a] |
|---|---|---|---|---|---|
| | | $X\ ^1\Sigma^+$ State | | | |
| $^7$LiH | 20287.7 ± 0.3 | 19589.8 ± 0.3 | 1.595584 | | VID 84, CHA 86 |
| $^7$LiD | 20293.5 ± 0.3 | 19768.8 ± 0.3 | 1.595304 | | VID 84, CHA 86 |
| $^6$LiH | 20287.7 ± 0.4 | 19582.6 ± 0.4 | 1.595584 | | VID 82, CHA 86 |
| $^6$LiD | 20293.5 ± 0.4 | 19759.2 ± 0.4 | 1.595304 | | VID 82, CHA 86 |
| | | $A\ ^1\Sigma^+$ State | | | |
| $^7$LiH | 8681.6 ± 0.3 | 8550.3 ± 0.3 | 2.59628 | 26509.77 | VID 82, VID 84 |
| $^7$LiD | 8684.7 ± 0.3 | 8587.8 ± 0.3 | 2.59690 | 26512.52 | VID 82, VID 84 |
| $^6$LiH | 8681.6 ± 0.4 | 8548.8 ± 0.4 | 2.59647 | 26509.68 | VID 82 |
| $^6$LiD | 8684.7 ± 0.4 | 8585.9 ± 0.4 | 2.59710 | 26512.44 | VID 82 |
| | | $B\ ^1\Pi$ State | | | |
| $^7$LiH | 288.9 ± 0.3 | 175.4 ± 0.3 | 2.3834 | 34902.48 | VID 84 |
| $^7$LiD | 291.1 ± 0.3 | 202.9 ± 0.3 | 2.3821 | 34906.13 | VID 84 |
| $^6$LiH | 288.9 ± 0.4 | 174.4 ± 0.4 | 2.3834 | 34902.5 | VID 84 |
| $^6$LiD | 291.1 ± 0.4 | 201.4 ± 0.4 | 2.3821 | 34906.1 | VID 84 |

[a]Values of $D_e$, $R_e$ and $T_e$ are from listed references; $D_0$ values are based on ZPEs calculated with adiabatically corrected $Y_{ij}$ (see Tables 5–7). For the $B\ ^1\Pi$ state, $D_0 = D_e - E(v=0, J=1)$; $E(0,1)$ is based on adiabatically corrected potential curve [VID 84].

TABLE 3. Laser coincidences of lithium hydride isotopomers in the $A$-$X$ band system

| Species | $\lambda_{laser}$(Å) | Exciting transition $(v',J' \leftarrow v'',J'')$ | $v_{max}$ | Ref. |
|---|---|---|---|---|
| $^7$LiH | 3345 | (16,9 ← 1,16) | 22 | STW 82 |
| $^7$LiD | 3514 | (14,10 ← 1,11) | 24 | ENN 81 |
| | 3638 | (10,6 ← 1,7) | 26 | ENN 81 |
| | 3358 | (19,22 ← 0,23) | 27 | STW 82 |
| | 3564 | (15,6 ← 2,5) | 17 | CHA 86 |
| | 3507 | (13,4 ← 1,3) | 16 | CHA 86 |
| $^6$LiH | 4579 | (5,10 ← 4,11) | 4 | ENN 81 |
| | 3336 | (12,10 ← 0,9) | 21 | VER 82 |
| $^6$LiD | 3507 | (15,17 ← 1,16) | 23 | CHA 86 |

The commonly defined vibrational energy $G(v)=\sum_{i=1} Y_{i0}(v+1/2)^i = Y_{10}(v+1/2)+ Y_{20}(v+1/2)^2+Y_{30}(v+1/2)^3+ ...=\omega_e(v+1/2)-\omega_e x_e(v+1/2)^2+\omega_e y_e(v+1/2)^3+...$ . The rotational constant $B_v=\sum_{i=0} Y_{i1}(v+1/2)^i = Y_{01}+Y_{11}(v+1/2) +Y_{21}(v+1/2)^2+...=B_e-\alpha_e(v+1/2)+\gamma_e(v+1/2)^2 + ...$ . However, in all our vibrational energy levels we also include with $G(v)$ the small $Y_{00}$ correction, as well as in the zero point energy ZPE (see footnotes, Table 4). $T_e$ is the electronic energy calculated from the minimum of the potential well of the $X\ ^1\Sigma^+$ ground state to the minimum of the potential well of the excited state. The dissociation energy $D_0$ is defined as the energy of the separated atoms relative to the lowest existing level ($v=0$, $J=0$ for the $X\ ^1\Sigma^+$ and $A\ ^1\Sigma^+$ states and $v=0$, $J=1$ for the $B\ ^1\Pi$ state) of the molecule. The ZPE and $D_e$ are defined with respect to the minimum of the potential well; hence $D_e=D_0+\text{ZPE}$.

Note that only three electronic states of LiH have been observed: the $X\ ^1\Sigma^+$ state correlating to Li + H, and the $A\ ^1\Sigma^+$ and $B\ ^1\Pi$ states correlating to Li ($2p\ ^2P^0$) + H. Many other singlet states correlating to higher asymptotes have been calculated theoretically (see Sec. 2.6). No triplet states have been observed but again there are theoretical calculations (Sec. 2.6).

Finally, the atomic and ionic fragments of LiH are well known energetically, not only in nonrelativistic *ab initio* quantum theory, but also including relativistic, radiative and other small corrections. For this reason, a separate Sec. 5 has been appended to precisely define the isotopic fragment energetics.

## 1.2. Glossary

| | |
|---|---|
| $A_v$ | Einstein $A$ coefficient |
| ad | adiabatic |
| α | polarizability; fine structure constant |
| CASSCF | complete active space SCF |
| CC | coupled cluster method |
| CCSD | coupled cluster single and double excitations |
| CEPA | coupled electron pair approximation |
| CI | configuration interaction (or superposition of configurations) |
| CSF | configuration state function |
| $D(R)$ | electronic transition dipole moment function |
| $E^{CR}$ | relativistic correction to the Coulomb energy |
| $E^Q$ | quantum electrodynamic corrections in the Lamb shift |

TABLE 4. Dunham coefficients $Y_{ij}$ (cm$^{-1}$) for $X\ ^1\Sigma^+$ state of $^7$LiH

| ZPE[a] | $Y_{00}$[a] | $Y_{10}$ | $Y_{20}$ | $Y_{30}$ | $Y_{40}$ | $Y_{01}$ | $Y_{11}$ | $10^3Y_{21}$ | $10^4Y_{31}$ | Ref. |
|---|---|---|---|---|---|---|---|---|---|---|
| 697.91 | 0.870 | 1405.649 | −23.200 | 0.1633 | | 7.5131 | −0.2131 | 0.75 | | CRA 35A |
| 697.97 | 0.931 | 1405.629 | −23.1950 | 0.16333 | | 7.5133 | −0.21514 | 1.5671 | | LI 78 |
| 698.13 | 0.865 | 1406.24 | −23.5505 | 0.24174 | −0.0068 | 7.5134 | −0.21582 | 1.977 | −0.48 | ORT 79 |
| 697.96 | 0.985 | 1405.444[b] | −23.091[b] | 0.1442[b] | 0.00168[b] | 7.51429[b] | −0.21616[b] | 1.776[b] | 0.2901[b] | VID 82[c] |
| | | | | | | 7.513784[b] | −0.21651[b] | 2.0398[b] | | PLU 84 |
| 697.94 | 1.061 | 1405.07781[b] | −22.68035[b] | −0.059985[b] | 0.0539595[b] | 7.513395[b] | −0.215263[b] | 0.87512[b] | 4.84325[b] | CHA 86[d] |
| 697.94 | 0.983 | 1405.45052[b] | −23.11863[b] | 0.153191[b] | | 7.51369847[b] | −0.2162784[b] | 1.9235[b] | | YAM 88 |
| 697.95 | 0.973 | 1405.50936[b] | −23.17938[b] | 0.176365[b] | −0.0029616[b] | 7.51375104[b] | −0.21646060[b] | 2.08653[b] | −0.44069[b] | MAK 90 |

[a] $\text{ZPE}=G(0)+Y_{00}$ where $G(0)=\frac{Y_{10}}{2}+\frac{Y_{20}}{4}+\frac{Y_{30}}{8}+\frac{Y_{40}}{16}+...$

and $Y_{00}=\frac{Y_{01}}{4}-\frac{Y_{11}Y_{10}}{12Y_{01}}+\frac{Y_{11}^2Y_{10}^2}{144Y_{01}^3}+\frac{Y_{20}}{4}$

[b] Dunham coefficients that include adiabatic corrections.

[c] $Y_{50}=-2.6091\times10^{-4}$ and $Y_{41}=-5.3614\times10^{-6}$.

[d] $Y_{i0}$ (with $i=5\rightarrow9$) and $Y_{i1}$ (with $i=4\rightarrow9$) are given in Table 5.

| | |
|---|---|
| $E^{FS}$ | finite nuclear size correction in the Lamb shift |
| $E^{CN}$ (NP) | nonrelativistic Coulomb energy |
| $E^{R}$ (RP) | relativistic Coulomb energy |
| $E^{Q}$ (QP) | relativistic Coulomb energy with quantum electrodynamic corrections |
| $E^{Q}$ (QF) | relativistic Coulomb energy with quantum electrodynamic corrections and finite nuclear size corrections |
| EA | electron affinity (adiabatic or vertical) |
| EOM | equations of motion |
| $eqQ$ | quadrupole coupling constant |
| $f$ | oscillator strength |
| FSGO | floating spherical Gaussian orbital |
| GTO | Gaussian-type orbital |
| GVB | generalized valence bond |
| HF | Hartree-Fock |
| IP | ionization potential |
| MBPT | many body perturbation theory |
| MCSCF | multiconfiguration SCF |
| MCTDHF | multiconfiguration time dependent Hartree-Fock |
| MO | molecular orbital |
| MRCI | multireference CI |
| MRSDCI | multireference singles and doubles CI |
| $\mu$ | dipole moment; reduced mass |
| $\mu(R)$ | dipole moment function |
| NO | natural orbital |
| NP | nonrelativistic, point nucleus |
| Num | numerical |
| PNO | pseudonatural orbital |
| PT | perturbation theory |
| $q$ | electric field gradient |
| $Q$ | quadrupole moment |
| QF | quantum electrodynamic, finite size nucleus |
| QMC | quantum Monte Carlo |
| QP | quantum electrodynamic, point nucleus |
| $R$ | internuclear distance |
| $R_\infty$ | Rydberg constant for infinite nuclear mass |
| RP | relativistic, point nucleus |
| SCF | self-consistent field approximation |
| SDO | shielded diatomic orbital |
| STO | Slater-type orbital |
| $\tau_v$ | lifetime |
| TDO | truncated diatomic orbital |
| $U(R)$ | potential energy function |
| UHF | unrestricted Hartree-Fock |
| vert | vertical |
| $V(R)$ | potential energy function |
| VB | valence bond |
| $\zeta$ | STO nonlinear parameter (zeta) |
| $Z$ | nuclear charge |
| ZPE | zero point energy |

## 2. Experimental and Theoretical Results

### 2.1. Conventional Spectroscopy

The first observation of $A\ ^1\Sigma^+$–$X\ ^1\Sigma^+$ band spectra of $^6$LiH and $^7$LiH was made by Nakamura [NAK 30, NAK 31]; emission and absorption bands with a dispersion of 2.3 Å/mm were reported. For $^7$LiH the bands involved transitions from $v'' = 0$–2 to various $v' = 1$–15 vibrational levels. Crawford and Jorgensen reported high resolution absorption spectra (1 Å/mm dispersion) for $^7$LiD ($v'' = 0$–3 to $v' = 1$–15) [CRA 35] and $^7$LiH ($v'' = 0$–2 to $v' = 1$–18) [CRA 35A]. Klemperer [KLE 55] observed rotation-vibration transitions in the infrared, but details were sparse. Anomalous behavior in several $A$–$X$ bands (e.g., 11–0 and 12–0 bands) was highlighted by Fernandez-Florez [FER 69]. Velasco and Rivero [VEL 74A] reported improved absorption band spectra (1.3 Å/mm) for $^6$LiH.

High resolution emission spectra for all isotopic combinations were reported by Li and Stwalley [LI 78]; they extended the $^7$LiH vibrational levels to $v'' = 3$–5 for the $X\ ^1\Sigma^+$ state and to $v' = 0$ for the $A\ ^1\Sigma^+$ state, and refitted lines identified by Crawford and Jorgensen. The $^7$LiH emission spectra of Orth and Stwalley [*ORT* 79] extended the $X$ state to $v'' = 12$ and provided further data on the $v' = 0$ level of the $A$ state where anomalous behavior is particularly strong. Rafi *et al.* [RAF 83] reported observations and analysis of five new rotation-vibration absorption bands for $^7$LiH where $v' = 16$–20.

Velasco [VEL 57] reported absorption spectra of $^7$LiH and $^7$LiD in the near ultraviolet explained by a new $B\ ^1\Pi$–$X\ ^1\Sigma^+$ band system; $P$, $Q$ and $R$ branches for (0–0), (1–0), (2–0), (0–1), (1–1) and (2–1) bands were tabulated. All bands showed a clear breaking off of rotational structure, explained by the rapid onset of predissociation with increasing $J$ in the extremely shallow upper $B\ ^1\Pi$ state. Stwalley *et al.* [STW 74] reexamined the $B$–$X$ absorption spectrum [VEL 57] and found four lines of the (3–1) band in $^7$LiD. In addition, Velasco reported a strong continuum to the short wavelength side of the $B$-$X$ band, corresponding to transition from the bottom of the ground state to the repulsive inner wall of the $B$ state [VEL 57]. Later he presented the actual continuum spectrum (with maximum intensity near 2700 Å) [VEL 74].

Pure rotation spectra in the ground state were studied first by Pearson and Gordy [PEA 69] in $^6$LiD and $^7$LiD ($J = 0$ and 1, $v = 0$ and 1) and more recently by Plummer *et al.* [PLU 84] in $^6$LiH ($J = 0$ and 1, $v = 0$), $^7$LiH ($J = 0$ and 1, $v = 0$ and 1), $^6$LiD ($J = 1$ and 2, $v = 0$) and $^7$LiD ($J = 1$ and 2, $v = 0$ and 1).

### 2.2. Laser Spectroscopy

Wine and Melton [WIN 76, MEL 77] employed laser-induced fluorescence excitation of $^7$LiH in a heat pipe oven to study collisions of the $A$ state. They showed that

quenching rates of LiH $A\ ^1\Sigma^+$ ($v' = 5$ or 6, $J'$) by ground state Li atoms were quite state specific [IBB 81]. Dagdigian [DAG 76] observed several $A$–$X$ laser-induced fluorescence excitation spectra in a supersonic molecular beam containing $^7$LiH and $^6$LiH. He used this laser fluorescence technique to study rotational [DAG 80A] and vibrational [DAG 80] energy transfer of LiH with a number of scattering partners. With laser-induced fluorescence, Dagdigian was also able to measure the electric dipole moment $\mu_v$ for different vibrational levels of the $A\ ^1\Sigma^+$ state [DAG 80B]. The above work is reviewed in [DAG 83]. Brieger *et al.* [BRI 80, BRI 83] applied the technique of laser-induced Stark quantum beats to the $A$ state levels $v' = 2$, 4 and 5, $J' = 1$ ($^7$LiH) and $v' = 6$, $J' = 1$ ($^7$LiD) to obtain experimental dipole moments of the $A$ state.

Stwalley and coworkers used argon ion laser-induced fluorescence experiments to produce long $v''$ progressions of $P$ and $R$ doublets [STW 82, VER 82, CHA 86]. Fluorescence lines in $^6$LiH ($A$–$X$) were excited by the argon ion 3336 Å laser line [VER 82]; the $v''$ range started at $v'' = 0$ and continued all the way to $v'' = 21$ (covering 99% of the $X$ state well). In $^7$LiD, Ennen and Ottinger [ENN 75] used the 3514 Å exciting line to obtain a 17-member series with $v'_{max} = 20$, and the 3638 Å line to obtain a 19-member series with $v'_{max} = 19$. Later they [ENN 81] used the 3514 Å and 3638 Å lines to reach $v'_{max} = 24$ and 26, respectively; [STW 82] reached $v'_{max} = 27$ with the 3358 Å line. In $^7$LiH, [STW 82] reached $v'_{max} = 22$ with the 3345 Å line. Chan *et al.* [CHA 86] investigated three krypton ion laser-induced fluorescence series: $^6$LiD (3507 Å) with $v'_{max} = 23$ and $^7$LiD (3507 Å and 3564 P) with $v'_{max} = 16$ and 17, respectively. Table 3 lists the exciting transitions for argon ion and krypton ion laser coincidences in the lithium hydride isotopomers. Von Moers *et al.* [VON 87] reported 69 lines of the $A$–$X$ (21–0), (22–0) and (23–0) bands for $^7$LiH.

Von Moers *et al.* [VON 87] also observed the same $B$-$X$ bands reported by Velasco [VEL 57] by the technique of delayed coincidence of molecular fluorescence in a molecular beam. Resonance fluorescence series in the $B$-$X$ band system were observed for the first time by Luh *et al.* [LUH 88]; six series of $^7$LiD and eight series of $^6$LiH were excited by a frequency-doubled dye laser pumped by a frequency-doubled YAG laser.

Highly accurate infrared diode laser spectroscopy was employed by Yamada and Hirota [YAM 88] to study over 40 rotation-vibration transitions: (1–0) band lines were observed for all four isotopic combinations; (2–1) band lines were observed for $^7$LiH, $^7$LiD and $^6$LiD; and (3–2) band lines were observed for $^7$LiD. Maki *et al.* [MAK 90] recorded spectra for high $J$ rotation-vibration and pure rotation transitions for all four isotopic combinations with a tunable diode laser and with a Fourier transform spectrometer; their infrared measurements are more extensive than those of [YAM 88]. A recent review of microwave and infrared spectra (including LiH) should be noted [HIR 92].

### 2.3. Spectroscopic Constants

The first report of vibrational and rotational spectroscopic constants was that of Crawford and Jorgensen [CRA 35, CRA 35A] for $^7$LiD and $^7$LiH for both the $X\ ^1\Sigma^+$ and the $A\ ^1\Sigma^+$ states. They also determined vibrational constants for the $X$ and the $A$ states of $^7$LiH based on the published results of Nakamura [NAK 30, NAK 31]; those constants were in good agreement with their own for the ground state [CRA 35A]. Based on microwave measurements, Pearson and Gordy [PEA 69] determined precise rotational constants for the ground state of $^6$LiD and $^7$LiD. Velasco and Rivero [VEL 74A] determined vibrational and rotational constants for both the $X$ and the $A$ states of $^6$LiH. Complete sets of spectroscopic constants of the $X$ and $A$ states for all four lithium hydride isotopomers were reported by Li and Stwalley [LI 78]; their $^7$LiH and $^7$LiD results included reanalysis of earlier data [CRA 35, CRA 35A].

Based on newly observed vibrational levels, Ennen and Ottinger [ENN 75] determined new spectroscopic constants for the $X$ state of $^7$LiD. In addition to increasing the measurement accuracy, they later [ENN 81] extended the wavelength range to include vibrational levels up to $v'_{max} = 26$; they reported improved Dunham coefficients for $X$ and $A$ states of $^7$LiD. The constants of Orth and Stwalley [ORT 79] on $^7$LiH were based on new $A$–$X$ data which extended the ground state to $v'' = 12$. Vidal and Stwalley [VID 82] reported adiabatically corrected spectroscopic constants for the $A$ and $X$ states of $^7$LiH, $^7$LiD, $^6$LiH and $^6$LiD. Chan *et al.* [CHA 86] reported improved adiabatically corrected spectroscopic constants, using new laser-induced fluorescence experiments for $^7$LiH, $^7$LiD and $^6$LiH; the expanded data field extended the vibrational levels from $v'_{max} = 15$ to $v'_{max} = 22$ for $^7$LiH and from $v'_{max} = 18$ to $v'_{max} = 27$ for $^7$LiD, for example.

Based on rotational spectra for all four isotopic combinations, Plummer *et al.* [PLU 84] reported precise rotational constants for the ground state of $^7$LiH; they included a Born-Oppenheimer correction, but only for the dominant rotational constant $Y_{01}$. High resolution infrared diode laser [YAM 88] and Fourier transform [MAK 90] spectroscopy yielded very precise adiabatically corrected constants for all four isotopomers of the ground state.

Rotational and vibrational constants for the $B\ ^1\Pi$ state ($^7$LiH and $^7$LiD) were first reported by Velasco [VEL 57]; even though analysis was limited, there was evidence of $\Lambda$ doubling. Based on a few more $B$-$X$ transitions, Stwalley *et al.* [STW 74] extended the $B$ state constants for $^7$LiD. Vidal and Stwalley [VID 84] give formulas to determine isotopically corrected spectroscopic constants for all four isotopomers in the $B$ state.

Assuming the Born-Oppenheimer separation of electronic and nuclear motions, the term values are written in the familiar Dunham expansion [HER 50]: $T_{vJ} = \Sigma\ Y_{ij}(v+1/2)^i[J(J+1)-\Lambda^2]^j$, where the $Y_{ij}$'s are the Dunham or spectroscopic constants. For the $^1\Sigma^+$ states, $\Lambda^2 = 0$; for the $^1\Pi$ state, $\Lambda^2 = 1$. At this level of approx-

imation one can use two different isotopic combinations and the familiar equation $Y_{ij}{}^{a}/Y_{ij}{}^{b} = [\mu^{b}/\mu^{a}]^{(i+2j)/2}$ [HER 50, STW 75] to determine spectroscopic constants of one isotopomer from those of another (the superscripts a and b refer to two isotopically distinct molecules). Thus several literature references contain lists of spectroscopic constants for several isotopomers based on the spectrum of only one isotopomer (e.g., [VEL 74A] using $^{6}$LiH).

A closely related approach for the determination of spectroscopic constants for lithium hydride is the use of the concept of mass-reduced quantum numbers. Within the Born-Oppenheimer approximation, the term values can be recast [WAY 73, STW 75, LI 79] as $T_{vJ} = \Sigma\, Y_{ij}\, \eta^{i}\xi^{j}$, where $\eta$ and $\xi$ are the vibrational and rotational mass-reduced quantum numbers, respectively: $\eta = (v+1/2)\mu^{-1/2}$ and $\xi = [J(J+1)-\Lambda^{2}]\mu^{-1}$. The use of mass-reduced quantum numbers permits one to combine spectroscopic data from each of several isotopomers to construct an improved isotopically combined potential energy curve. The point here is to recognize the benefit of combining data for several isotopic variants to obtain improved $T_{vJ}$ (and potential energy curve) results. The accurate determination of the very shallow potential energy curve of the $B\ ^{1}\Pi$ state of lithium hydride [WAY 73] and the characterization of an unusual flat shoulder in the outer limb of the potential curve of the $X\ ^{2}\Sigma^{+}$ state of mercury hydride [STW 75] are two especially successful applications of mass-reduced quantum numbers.

Table 4 contains a comparison and chronology of the spectroscopic constants found in the literature for the ground state of $^{7}$LiH directly. Constants for $^{7}$LiH obtained indirectly from another isotopomer (via the reduced mass relationship just noted) are not included. The most remarkable feature that emerges from the tabulation is the near constancy of the values of the leading two vibrational and two rotational constants since the original Crawford and Jorgensen report over 55 years ago [CRA 35A]. This is noteworthy because the most recent determinations (since 1982) are the $Y_{ij}^{(0)}$ "Dunham-type coefficients", not the more common $Y_{ij}$ "Dunham coefficients". The distinction between these two different coefficients is easily understood if each $Y_{ij}$ Dunham coefficient is expanded as a series of contributions [DUN 32, SAN 38, SAN 39, SAN 40, STW 75, OGI 87, OGI 90] $Y_{ij} = Y_{ij}^{(0)} + Y_{ij}^{(1)} + Y_{ij}^{(2)} + \ldots\ldots$, where $= Y_{ij}^{(0)}$ is the result of the first-order quantization condition of the WKB method [COX 86] and the higher order contributions get progressively smaller in magnitude. Only for the first-order quantization approximation, are the "classical" and "mechanical" $Y_{ij}^{(0)}$ Dunham-type coefficients equivalent to the common molecular constants ($Y_{10}^{(0)} = \omega_e$, $Y_{20}^{(0)} = -\omega_e x_e$, $Y_{01}^{(0)} = B_e$, $Y_{11}^{(0)} = -\alpha_e$, etc.) and the (0) superscript is unfortunately routinely omitted.

In precision lithium hydride work, the higher order contributions to $Y_{ij}$ should not be omitted because (i) higher order terms in the WKB semiclassical quantization condition are not negligible and (ii) the breakdown of the Born-Oppenheimer approximation is important. Instead of the expression $Y_{ij} = Y_{ij}^{(0)} + Y_{ij}^{(1)} + \ldots$, for the heteronuclear lithium hydride molecule, the Dunham coefficient expansion can be replaced by the nearly equivalent expression due to Watson [WAT 73, WAT 80]: $Y_{ij} = Y_{ij}^{(0)}[1 + m_e(\Delta_{ij}^{H}/M_H + \Delta_{ij}^{Li}/M_{Li}) + \ldots]$, where $m_e$ is the electron mass, $M_H$ and $M_{Li}$ are the atomic masses of the H and Li isotopes, and the mass-invariant correction parameters $\Delta_{ij}^{H,Li}$ take into account second-order energy coefficients $Y_{ij}^{(1)}$ as well as adiabatic effects [WAT 80, OGI 90]. Values for these non-Born-Oppenheimer correction factors can be found in recent reports [PLU 84, YAM 88, MAK 90].

Vidal and Stwalley [VID 82] employed the term value expansion $T_{vJ} = \Sigma \bar{A}_{ij}(v+1/2)^{i}[J(J+1)-\Lambda^{2}]^{j}\,\mu_r^{-(i+2j)/2}$, with $\bar{A}_{ij} = A_{ij} + B_{ij}^{H}/M_H + B_{ij}^{Li}/M_{Li}$ (higher order corrections are too small to characterize experimentally) and the relative reduced mass $\mu_r = \mu/\mu(^{7}\text{LiH})$. Their approach to Dunham-type coefficients is equivalent to that described in the preceding paragraphs, i.e. the complete $Y_{ij} = \bar{A}_{ij}\,\mu_r^{-(i+2j)/2}$. In this approach [VID 82, VID 84, CHA 86], data for all isotopic combinations are used simultaneously to determine each set of $A_{ij}$, $B_{ij}^{H}$ and $B_{ij}^{Li}$ Dunham-type coefficients.

In Table 4, small differences between the constants of [LI 78] and [ORT 79] can be accounted for by the fact that [LI 78] include data up to $v'_{max} = 5$ while [ORT 79] go to $v'_{max} = 12$. Similarly, the small differences between the earlier adiabatically corrected constants of [VID 82] and the improved ones of [CHA 86] are because [CHA 86] expanded considerably the field of data, which includes the ionic-covalent avoided crossing region of the $X\ ^{1}\Sigma^{+}$ state potential energy curve.

The results of [MAK 90] are based on spectra involving only the low-lying levels in the potential well; their very precise constants are recommended for vibrational levels $v \leq 3$ of the $X\ ^{1}\Sigma^{+}$ state (see Table 5). The constants of [CHA 86] are recommended for higher levels of the $X\ ^{1}\Sigma^{+}$ state and for the $A\ ^{1}\Sigma^{+}$ state; see Tables 5 and 6, respectively. The constants of [VID 84] are recommended for the $B\ ^{1}\Pi$ state; see Table 7. Note that only $Y_{i0}$ and $Y_{i1}$ coefficients are tabulated here as these determine the potentials; see the original references for the uncertainties in these coefficients and for the higher order coefficients $Y_{ij}(j \geq 2)$.

Contrary to the situation with the other alkali hydrides [STW 91], for lithium hydride the zero point energy of the $A\ ^{1}\Sigma^{+}$ state is well characterized experimentally and the uncertainty in $T_e$ for the $A$ state is small ($< 1.0\ cm^{-1}$). Reported values for $T_e$ are [VID 82]: 26,509.77 $cm^{-1}$ ($^{7}$LiH), 26,512.52 $cm^{-1}$ ($^{7}$LiD), 26,509.68 $cm^{-1}$ ($^{6}$LiH) and 26,512.44 $cm^{-1}$ ($^{6}$LiD). Note that the change in going from H to D is significant, but the change in going from $^{6}$Li to $^{7}$Li is very small ($\leq 0.1\ cm^{-1}$).

For the $B\ ^{1}\Pi$ state, $T_e$ values are [VID 84]: 34,902.48 $cm^{-1}$ ($^{7}$LiH) and 34,906.13 $cm^{-1}$ ($^{7}$LiD). Because adiabatic corrections have only been reported for the hydrogen atom and not for the lithium atom in the case of the $B$ state [VID 84], within experimental uncertainties $T_e(^{6}\text{LiH}) = T_e(^{7}\text{LiH})$ and $T_e(^{6}\text{LiD}) = T_e(^{7}\text{LiD})$. The

TABLE 5. Recommended spectroscopic constants $Y_{ij}$ (Dunham coefficients[a]) for $j = 0$ and 1 for the $X\,^1\Sigma^+$ state of the lithium hydrides and deuterides (in $cm^{-1}$). The upper entries are from [MAK 90]; the lower entries are from [CHA 86]. The [MAK 90] constants are based on $v \leq 3$ levels while the [CHA 86] constants are based also on higher $v$ levels[b]

| | [MAK 90] $v \leq 3$ | | | |
|---|---|---|---|---|
| | $^7$LiH | $^7$LiD | $^6$LiH | $^6$LiD |
| $Y_{10}$ | 1405.50936 | 1054.93684 | 1420.11754 | 1074.33199 |
| $Y_{20}$ | −23.17938 | −13.05489 | −23.66382 | −13.53939 |
| $Y_{30}$ | 0.176365 | 0.074531 | 0.181923 | 0.078718 |
| $10^1Y_{40}$ | −0.029616 | −0.009392 | −0.030867 | −0.010102 |
| $Y_{01}$ | 7.51375104 | 4.23307991 | 7.67077500 | 4.39017570 |
| $Y_{11}$ | −0.21646060 | −0.09149367 | −0.22328190 | −0.096634 |
| $10^2Y_{21}$ | 0.208653 | 0.066169 | 0.217465 | 0.071171 |
| $10^3Y_{31}$ | −0.044069 | −0.010487 | −0.046407 | −0.011488 |
| | [CHA 86] $v > 3$ | | | |
| $Y_{10}$ | 1405.07781 | 1055.00696 | 1419.68479 | 1074.40587 |
| $Y_{20}$ | −22.68035 | −13.18954 | −23.15436 | −13.67905 |
| $Y_{30}$ | −0.059985 | 0.161683 | −0.061875 | 0.170767 |
| $10^1Y_{40}$ | 0.539595 | −0.271594 | 0.562386 | −0.292128 |
| $10^2Y_{50}$ | −0.77313 | 0.40715 | −0.81416 | 0.44598 |
| $10^3Y_{60}$ | 0.61554 | −0.34452 | 0.65495 | −0.38432 |
| $10^4Y_{70}$ | −0.28930 | 0.15974 | −0.31102 | 0.18147 |
| $10^6Y_{80}$ | 0.72552 | −0.38406 | 0.78811 | −0.44433 |
| $10^8Y_{90}$ | −0.78559 | 0.37152 | −0.86223 | 0.43772 |
| $Y_{01}$ | 7.513395 | 4.233182 | 7.670410 | 4.390281 |
| $Y_{11}$ | −0.215263 | −0.091882 | −0.222047 | −0.097044 |
| $10^2Y_{21}$ | 0.087512 | 0.114487 | 0.091208 | 0.123250 |
| $10^3Y_{31}$ | 0.484325 | −0.279880 | 0.510028 | −0.306576 |
| $10^3Y_{41}$ | −0.11897 | 0.07382 | −0.12659 | 0.08235 |
| $10^4Y_{51}$ | 0.15080 | −0.10842 | 0.16212 | −0.12317 |
| $10^5Y_{61}$ | −0.11054 | 0.08867 | −0.12007 | 0.10259 |
| $10^7Y_{71}$ | 0.43603 | −0.40546 | 0.47856 | −0.47771 |
| $10^9Y_{81}$ | −0.80190 | 0.96740 | −0.88928 | 1.1607 |
| $10^{11}Y_{91}$ | 0.32425 | −0.94340 | 0.36332 | −1.1528 |

[a] Reported constants include adiabatic contributions.

[b] The alternation in sign of higher order coefficients ($Y_{no}$ and $Y_{n1}$, $n \rangle 3$) between hydrides and deuterides is correct since the $A_{ni}$ and $B_{ni}^{H}$ coefficients [CHA86] are comparable in magnitude and opposite in sign.

angular momentum quantum number $\Lambda = 1$ for the $B$ state and $\Lambda$-type doubling [HER 50] has been observed in the $B$–$X$ system [VEL 57]. The magnitude of the splitting is quite small; the only statistically significant term characterizing the $\Lambda$-type doubling is the $a_{01}[J(J+1)-\Lambda^2]$ term defined in [VID 84] ($a_{01} = 0.002\ cm^{-1}$ for $^7$LiH and $0.001\ cm^{-1}$ for $^7$LiD).

TABLE 6. Recommended spectroscopic constants $Y_{ij}$ (Dunham coefficients[a] [CHA 86]) for $j = 0$ and 1 for the $A\,^1\Sigma^+$ state of the lithium hydrides and deuterides (in $cm^{-1}$)

| | $^7$LiH | $^7$LiD | $^6$LiH | $^6$LiD |
|---|---|---|---|---|
| $Y_{10}$ | 234.50825 | 178.57167 | 236.93379 | 181.84580 |
| $Y_{20}$ | 28.81350 | 15.31830 | 29.41569 | 15.88681 |
| $Y_{30}$ | −4.203237 | −1.603727 | −4.335693 | −1.693829 |
| $Y_{40}$ | 0.555530 | 0.157664 | 0.578994 | 0.169584 |
| $10^1Y_{50}$ | −0.558553 | −0.121731 | −0.588196 | −0.133341 |
| $10^2Y_{60}$ | 0.374676 | 0.063362 | 0.398663 | 0.070682 |
| $10^3Y_{70}$ | −0.156418 | −0.020504 | −0.168162 | −0.023293 |
| $10^5Y_{80}$ | 0.364606 | 0.036668 | 0.396055 | 0.042422 |
| $10^7Y_{90}$ | −0.360095 | −0.027176 | −0.395222 | −0.032019 |
| $Y_{01}$ | 2.800056 | 1.588622 | 2.858445 | 1.657505 |
| $Y_{11}$ | 0.120800 | 0.040008 | 0.124607 | 0.042256 |
| $10^1Y_{21}$ | −0.620590 | −0.153623 | −0.646801 | −0.165238 |
| $10^1Y_{31}$ | 0.189547 | 0.036582 | 0.203778 | 0.040071 |
| $10^2Y_{41}$ | −0.361620 | −0.055229 | −0.384771 | −0.061609 |
| $10^3Y_{51}$ | 0.423932 | 0.051055 | 0.455761 | 0.058000 |
| $10^4Y_{61}$ | −0.305196 | −0.028834 | −0.331521 | −0.033359 |
| $10^5Y_{71}$ | 0.130228 | 0.009584 | 0.142932 | 0.011291 |
| $10^7Y_{81}$ | −0.297886 | −0.016870 | −0.330343 | −0.020242 |
| $10^9Y_{91}$ | 0.274883 | 0.011682 | 0.308003 | 0.014275 |

[a] Reported constants include adiabatic contributions.

TABLE 7. Recommended spectroscopic constants $Y_{ij}$ (Dunham coefficients[a] [VID 84]) for $j = 0$ and 1 for the $B\,^1\Pi$ state of the lithium hydrides and deuterides (in $cm^{-1}$)

| | $^7$LiH | $^7$LiD | $^6$LiH | $^6$LiD |
|---|---|---|---|---|
| $Y_{10}$ | 262.474 | 197.142 | 265.202 | 200.767 |
| $Y_{20}$ | −79.904 | −44.953 | −81.574 | −46.621 |
| $Y_{30}$ | 8.3028 | 3.5087 | 8.5644 | 3.7058 |
| $Y_{01}$ | 3.42817 | 1.92633 | 3.49982 | 1.99782 |
| $Y_{11}$ | −1.1030 | −0.45854 | −1.1377 | −0.48430 |
| $Y_{21}$ | 0.00838 | 0.00266 | 0.00873 | 0.00286 |

[a] Reported constants include adiabatic contributions.

## 2.4. Potential Energy Curves

The first RKR potential curves for the $X\,^1\Sigma^+$ and $A\,^1\Sigma^+$ states [FAL 60] were based on the spectroscopic data of [CRA 35A]; [FAL 60] did not include data for the $v' = 0$ level of the A state where anomalous behavior is strong. Singh and Jain [SIN 62, SIN 62A] reported an $A$ state RKR curve that was slightly different from the lowest three vibrational levels of [FAL 60]. Li and Stwalley [LI 78] obtained RKR curves for the four isotopomers $^7$LiH, $^7$LiD, $^6$LiH and $^6$LiD for $X$ and $A$ states; they included $v' = 0$ level data for the $A$ state of $^7$LiH and $^6$LiH. They also reported an isotopically combined RKR potential for the $X\,^1\Sigma^+$ state [LI 79]. An improved $^7$LiH $X$ state RKR curve was reported by [ORT 79]; they included the $Y_{00}$ term in the zero point energy (see footnotes, Table 4). Verma and Stwalley [STW 82, VER 82] constructed an RKR curve for the $^6$LiH $X$ state that covered over 99% of the potential well.

For the $B\ ^1\Pi$ state, [FAL 60] reported a very limited RKR curve ($v = 0$ and 1 only). Way and Stwalley [WAY 73] constructed a more complete isotopically combined RKR curve based on the isotopic variants $^7$LiH and $^7$LiD (see [ZEM 78B] for actual turning points).

Jenč and Brandt have repeatedly used their reduced potential curve (RPC) method to analyze and evaluate RKR curves for the alkali hydrides [JEN 66, JEN 85, JEN 86, JEN 91]. In the case of an incomplete or approximate potential energy curve (e.g., the ground state RKR curve of RbH covers only 66% of the well [STW 91]), the RPC analysis may be beneficial. However, for lithium hydride, where the potential energy curves of even the different isotopomers are already very reliably known, an RPC analysis provides little additional insight.

The step beyond the RKR potential energy curve is to include adiabatic corrections in the potential directly. The use of adiabatically corrected Dunham coefficients (which incorporate the effects of higher order WKB terms in the $Y_{ij}$'s) in the RKR inversion procedure does not wholly accomplish this goal [COX 86] because the procedure itself is a first-order quantization procedure. Within the adiabatic approximation, the corrected potential for lithium hydride is given by $U(R) = U_{BO}(R) + \Delta U^{H}(R)/M_H + \Delta U^{Li}(R)/M_{Li}$, where $U_{BO}(R)$ is the Born-Oppenheimer potential and $\Delta U^{H,Li}(R)$ are mass-invariant adiabatic corrections for the Born-Oppenheimer potential. Theoretical values of these adiabatic corrections have been calculated by several approaches [KLE 73, KLE 74, KLE 74A, BUN 77, BAR 78, BIS 83, BIS 83A, BIS 83B, HAD 86, OGI 87, JEN 88].

Vidal, Stwalley and coworkers [VID 82, VID 84, CHA 86] used the inverted perturbation approach (IPA) first proposed by [KOS 74] and developed by [VID 77]. The IPA method iteratively determines a correction to the potential energy by minimizing in a least square sense the difference between the experimental term energy $T_{v,J}$ and the calculated eigenvalue $E_{v,J} = \langle \Psi_{v,J} | H(R) | \Psi_{v,J} \rangle$, where $\Psi_{v,J}$ is the radial wave function for the Hamiltonian $H(R)$ corresponding to improved potential $U(R)$. Thus the local corrections to the potential energy curve are based variationally on a quantum mechanical energy eigenvalue numerical fit to measured line positions; the resulting potential energy curve is based solely on spectroscopic measurements, often with a global coverage. The recommended adiabatically corrected potential energy curves for $X\ ^1\Sigma^+$, $A\ ^1\Sigma^+$ and $B\ ^1\Pi$ states are found in Tables 8–12. The curves for the $X$ and $A$ states are tabulated according to the vibrational quantum number and are in a format used commonly for RKR potentials. Because the curve is very shallow for the $B$ state, there are only three or four vibrational levels and thus a more extensive curve is tabulated. The distances for the repulsive inner wall are closely spaced to properly characterize the steepness of the curve, while the outer attractive wall distances are widely spaced.

TABLE 8. IPA potential energy curves of $^7$LiH and $^7$LiD for the $X\ ^1\Sigma^+$ state [CHA86]

| | $^7$LiH | | | $^7$LiD | | |
|---|---|---|---|---|---|---|
| $v$ | $[G(v)+Y_{00}]^a$ | $R_-$(Å) | $R_+$(Å) | $[G(v)+Y_{00}]^a$ | $R_-$(Å) | $R_+$(Å) |
| 0 | 697.88 | 1.4456 | 1.7781 | 524.69 | 1.4637 | 1.7512 |
| 1 | 2057.59 | 1.3531 | 1.9367 | 1553.71 | 1.3807 | 1.8836 |
| 2 | 3372.48 | 1.2967 | 2.0607 | 2557.33 | 1.3292 | 1.9852 |
| 3 | 4643.37 | 1.2548 | 2.1717 | 3535.86 | 1.2905 | 2.0749 |
| 4 | 5871.14 | 1.2212 | 2.2760 | 4489.67 | 1.2592 | 2.1581 |
| 5 | 7056.58 | 1.1932 | 2.3764 | 5419.13 | 1.2327 | 2.2373 |
| 6 | 8200.35 | 1.1693 | 2.4747 | 6324.60 | 1.2099 | 2.3139 |
| 7 | 9302.95 | 1.1484 | 2.5721 | 7206.40 | 1.1897 | 2.3887 |
| 8 | 10364.73 | 1.1300 | 2.6692 | 8064.77 | 1.1718 | 2.4625 |
| 9 | 11385.90 | 1.1136 | 2.7670 | 8899.95 | 1.1556 | 2.5356 |
| 10 | 12366.42 | 1.0988 | 2.8660 | 9712.08 | 1.1409 | 2.6085 |
| 11 | 13306.04 | 1.0853 | 2.9669 | 10501.29 | 1.1275 | 2.6815 |
| 12 | 14204.13 | 1.0731 | 3.0706 | 11267.63 | 1.1152 | 2.7548 |
| 13 | 15059.61 | 1.0618 | 3.1781 | 12011.09 | 1.1038 | 2.8288 |
| 14 | 15870.80 | 1.0514 | 3.2908 | 12731.57 | 1.0933 | 2.9037 |
| 15 | 16635.24 | 1.0417 | 3.4106 | 13428.90 | 1.0834 | 2.9799 |
| 16 | 17349.46 | 1.0327 | 3.5401 | 14102.75 | 1.0742 | 3.0577 |
| 17 | 18008.73 | 1.0245 | 3.6835 | 14752.68 | 1.0656 | 3.1376 |
| 18 | 18606.62 | 1.0182 | 3.8473 | 15378.05 | 1.0575 | 3.2200 |
| 19 | 19134.53 | 1.0136 | 4.0424 | 15978.00 | 1.0498 | 3.3057 |
| 20 | 19581.14 | 1.0098 | 4.2897 | 16551.42 | 1.0425 | 3.3956 |
| 21 | 19932.13 | 1.0067 | 4.6331 | 17096.85 | 1.0356 | 3.4906 |
| 22 | 20169.84 | 1.0047 | 5.2049 | 17612.46 | 1.0291 | 3.5925 |
| 23 | | | | 18095.94 | 1.0232 | 3.7033 |
| 24 | | | | 18544.37 | 1.0186 | 3.8261 |
| 25 | | | | 18954.15 | 1.0149 | 3.9654 |
| 26 | | | | 19320.78 | 1.0118 | 4.1286 |
| 27 | | | | 19638.84 | 1.0091 | 4.3275 |

[a] In $cm^{-1}$.

TABLE 9. IPA potential energy curves of $^6$LiH and $^6$LiD for the $X\ ^1\Sigma^+$ state [CHA86]

| | $^6$LiH | | | $^6$LiD | | |
|---|---|---|---|---|---|---|
| $v$ | $[G(v)+Y_{00}]^a$ | $R_-$(Å) | $R_+$(Å) | $[G(v)+Y_{00}]^a$ | $R_-$(Å) | $R_+$(Å) |
| 0 | 705.08 | 1.4449 | 1.7791 | 534.29 | 1.4626 | 1.7528 |
| 1 | 2078.45 | 1.3520 | 1.9388 | 1581.75 | 1.3790 | 1.8867 |
| 2 | 3406.08 | 1.2955 | 2.0637 | 2602.88 | 1.3272 | 1.9896 |
| 3 | 4688.81 | 1.2534 | 2.1756 | 3598.00 | 1.2883 | 2.0805 |
| 4 | 5927.55 | 1.2198 | 2.2807 | 4567.51 | 1.2568 | 2.1648 |
| 5 | 7123.12 | 1.1918 | 2.3821 | 5511.80 | 1.2303 | 2.2452 |
| 6 | 8276.16 | 1.1678 | 2.4813 | 6431.25 | 1.2073 | 2.3229 |
| 7 | 9387.21 | 1.1469 | 2.5796 | 7326.17 | 1.1871 | 2.3990 |
| 8 | 10456.61 | 1.1285 | 2.6778 | 8196.84 | 1.1692 | 2.4740 |
| 9 | 11484.55 | 1.1120 | 2.7767 | 9043.48 | 1.1530 | 2.5484 |
| 10 | 12470.99 | 1.0973 | 2.8769 | | | |
| 11 | 13415.62 | 1.0838 | 2.9791 | | | |
| 12 | 14317.74 | 1.0716 | 3.0843 | | | |
| 13 | 15176.19 | 1.0603 | 3.1936 | | | |
| 14 | 15989.12 | 1.0499 | 3.3083 | | | |
| 15 | 16753.86 | 1.0402 | 3.4307 | | | |
| 16 | 17466.64 | 1.0312 | 3.5636 | | | |
| 17 | 18122.33 | 1.0232 | 3.7116 | | | |
| 18 | 18713.93 | 1.0172 | 3.8819 | | | |
| 19 | 19232.10 | 1.0128 | 4.0875 | | | |
| 20 | 19664.54 | 1.0090 | 4.3526 | | | |
| 21 | 19995.83 | 1.0062 | 4.7325 | | | |

[a] In $cm^{-1}$.

TABLE 10. IPA potential energy curves of $^7$LiH and $^7$LiD for the $A\ ^1\Sigma^+$ state [VID82]

| | $^7$LiH | | | $^7$LiD | | |
|---|---|---|---|---|---|---|
| $v$ | $[G(v)+Y_{00}]^a$ | $R_-$(Å) | $R_+$(Å) | $[G(v)+Y_{00}]^a$ | $R_-$(Å) | $R_+$(Å) |
| 0 | 131.26 | 2.2252 | 3.0087 | 96.33 | 2.2703 | 2.9538 |
| 1 | 412.28 | 2.0242 | 3.2831 | 300.56 | 2.0844 | 3.1955 |
| 2 | 725.25 | 1.9080 | 3.4685 | 525.17 | 1.9752 | 3.3578 |
| 3 | 1060.94 | 1.8244 | 3.6192 | 765.11 | 1.8960 | 3.4883 |
| 4 | 1413.74 | 1.7589 | 3.7514 | 1017.27 | 1.8333 | 3.6013 |
| 5 | 1779.57 | 1.7050 | 3.8724 | 1279.33 | 1.7814 | 3.7031 |
| 6 | 2155.19 | 1.6589 | 3.9864 | 1549.46 | 1.7370 | 3.7975 |
| 7 | 2537.91 | 1.6189 | 4.0960 | 1826.16 | 1.6982 | 3.8867 |
| 8 | 2925.47 | 1.5839 | 4.2029 | 2108.15 | 1.6636 | 3.9722 |
| 9 | 3315.89 | 1.5528 | 4.3082 | 2394.29 | 1.6326 | 4.0551 |
| 10 | 3707.44 | 1.5249 | 4.4130 | 2683.59 | 1.6045 | 4.1361 |
| 11 | 4098.53 | 1.4994 | 4.5180 | 2975.16 | 1.5790 | 4.2159 |
| 12 | 4487.70 | 1.4758 | 4.6239 | 3268.23 | 1.5557 | 4.2949 |
| 13 | 4873.61 | 1.4541 | 4.7314 | 3562.04 | 1.5342 | 4.3735 |
| 14 | 5274.97 | 1.4342 | 4.8410 | 3855.93 | 1.5143 | 4.4521 |
| 15 | 5630.47 | 1.4162 | 4.9538 | 4149.25 | 1.4955 | 4.5310 |
| 16 | | | | 4441.40 | 1.4778 | 4.6104 |
| 17 | | | | 4731.78 | 1.4612 | 4.6907 |
| 18 | | | | 5019.86 | 1.4456 | 4.7721 |

[a] In cm$^{-1}$.

TABLE 11. IPA potential energy curves of $^6$LiH and $^6$LiD for the $A\ ^1\Sigma^+$ state [VID82]

| | $^6$LiH | | | $^6$LiD | | |
|---|---|---|---|---|---|---|
| $v$ | $[G(v)+Y_{00}]^a$ | $R_-$(Å) | $R_+$(Å) | $[G(v)+Y_{00}]^a$ | $R_-$(Å) | $R_+$(Å) |
| 0 | 132.73 | 2.2236 | 3.0110 | 98.22 | 2.2677 | 2.9573 |
| 1 | 417.01 | 2.0220 | 3.2866 | 306.59 | 2.0808 | 3.2008 |
| 2 | 733.75 | 1.9056 | 3.4729 | 535.94 | 1.9711 | 3.3645 |
| 3 | 1073.51 | 1.8218 | 3.6244 | 781.03 | 1.8916 | 3.4961 |
| 4 | 1430.59 | 1.7562 | 3.7573 | 1038.63 | 1.8287 | 3.6102 |
| 5 | 1800.80 | 1.7022 | 3.8792 | 1306.31 | 1.7766 | 3.7131 |
| 6 | 2180.82 | 1.6561 | 3.9940 | 1582.20 | 1.7321 | 3.8085 |
| 7 | 2567.94 | 1.6161 | 4.1045 | 1864.74 | 1.6932 | 3.8988 |
| 8 | 2959.82 | 1.5810 | 4.2123 | 2152.59 | 1.6586 | 3.9854 |
| 9 | 3354.47 | 1.5499 | 4.3185 | 2444.58 | 1.6275 | 4.0695 |
| 10 | 3750.09 | 1.5220 | 4.4245 | 2739.68 | 1.5994 | 4.1517 |
| 11 | 4145.08 | 1.4965 | 4.5307 | 3036.98 | 1.5739 | 4.2327 |
| 12 | 4537.95 | 1.4730 | 4.6379 | 3335.65 | 1.5507 | 4.3130 |
| 13 | 4927.31 | 1.4512 | 4.7467 | 3634.93 | 1.5292 | 4.3930 |
| 14 | 5311.84 | 1.4314 | 4.8579 | 3934.13 | 1.5092 | 4.4731 |
| 15 | 5690.18 | 1.4134 | 4.9724 | 4232.56 | 1.4904 | 4.5536 |
| 16 | 6060.93 | 1.3969 | 5.0912 | 4529.60 | 1.4727 | 4.6348 |
| 17 | | | | 4824.64 | 1.4561 | 4.7169 |
| 18 | | | | 5117.10 | 1.4405 | 4.8002 |

[a] In cm$^{-1}$.

TABLE 12. IPA potential energy curves of lithium hydrides and deuterides forthe $B\ ^1\Pi$ state [VID 84]

| $R$(Å) | LiH $U$(cm$^{-1}$) | LiD $U$(cm$^{-1}$) |
|---|---|---|
| 1.94 | 372.84 | 371.24 |
| 1.96 | 327.56 | 326.06 |
| 1.98 | 287.39 | 285.99 |
| 2.00 | 251.67 | 250.37 |
| 2.02 | 223.80 | 222.60 |
| 2.04 | 196.51 | 195.40 |
| 2.06 | 170.00 | 168.97 |
| 2.08 | 145.24 | 144.29 |
| 2.10 | 122.65 | 121.78 |
| 2.15 | 76.18 | 75.50 |
| 2.20 | 43.15 | 42.65 |
| 2.25 | 21.35 | 21.00 |
| 2.30 | 8.20 | 7.99 |
| 2.35 | 1.35 | 1.27 |
| 2.38 | 0.01 | 0.005 |
| 2.41 | 0.59 | 0.66 |
| 2.45 | 3.41 | 3.57 |
| 2.50 | 9.47 | 9.73 |
| 2.55 | 17.55 | 17.90 |
| 2.60 | 27.00 | 27.44 |
| 2.65 | 37.33 | 37.85 |
| 2.70 | 48.19 | 49.79 |
| 2.75 | 59.35 | 60.02 |
| 2.80 | 70.61 | 71.36 |
| 2.85 | 81.74 | 82.55 |
| 2.90 | 92.60 | 93.47 |
| 2.95 | 103.11 | 104.04 |
| 3.00 | 113.22 | 114.19 |
| 3.20 | 149.03 | 150.18 |
| 3.40 | 177.61 | 178.90 |
| 3.60 | 199.96 | 201.37 |
| 3.80 | 217.38 | 218.89 |
| 4.00 | 231.02 | 232.61 |
| 4.50 | 254.03 | 255.76 |
| 5.00 | 267.58 | 269.41 |
| 5.50 | 275.79 | 277.68 |
| 6.00 | 280.81 | 282.76 |
| 6.50 | 283.80 | 285.78 |
| 7.00 | 285.54 | 287.55 |
| 8.00 | 287.31 | 289.36 |
| 9.00 | 288.10 | 290.18 |
| 10.00 | 288.50 | 290.59 |
| 11.00 | 288.69 | 290.80 |
| 12.00 | 288.79 | 290.90 |

The uncertainties in these potential energy curves are quite small [VID 82, VID 84, CHA 86], usually $<0.001$ Å and $<0.1$ cm$^{-1}$. An exception is the $B\ ^1\Pi$ state, for which the somewhat larger uncertainties are tabulated [VID 84]. A useful approximation in estimating uncertainties in the RKR turning points $\delta R_{v\pm}$ (based on uncertainties in the vibrational energy spacings $\delta\Delta G_{v-1/2}$ and rotational constants $\delta B_v$) is the semiclassical result of LeRoy [LER 70]:

$$\delta R_{v\pm} = \left[R_{v+} + R_{v-}\right]\left(\frac{\delta B_v}{4B_v}\right) + \left[R_{v+} - R_{v-}\right]\left(\frac{\delta\Delta G_{v-1/2}}{4\Delta G_{v-1/2}}\right)$$

Hybrid potential energy curves have been constructed for the $X\ ^1\Sigma^+$ state of LiH [STW 77, STW 82, VER 82, PAR 86, PAR 86B, PAR 88] and LiD [PAR 86B], the $A\ ^1\Sigma^+$ state of LiH [STW 77, PAR 86, PAR 86B, PAR 88] and LiD [PAR 86, PAR 86B, PAR 88], and the $B\ ^1\Pi$ state of $^7$LiH [WAY 73, ZEM 78B]. For the $^7$LiH $X$ state, the

[STW 77] curve utilizes the RKR curve of [FAL 60] up to $v'' = 3$ ($R_{3+} = 2.17$ Å), the *ab initio* points of [DOC 72] from 2.17–8.0 Å, and for $R > 8.0$ Å the long-range expansion $-C_6R^{-6} - C_8R^{-8} - C_{10}R^{-10}$ (where the $C_6$, $C_8$ and $C_{10}$ dispersion coefficients are based on multipole-multipole interactions [PRO 77]). For the $^7$LiH $A$ state, the [STW 77] curve utilizes the RKR curve [FAL 60] up to $v' = 13$ ($R_{13+} = 4.74$ Å), the *ab initio* points of [DOC 72] for 4.74–9.0 Å, and for $R > 9.0$ Å the long-range expansion $-C_6R^{-6} - C_8R^{-8}$ (with the dispersion coefficients of [PRO 77]). The inner walls for $X$ and $A$ states [STW 77] were linear extrapolations based on *ab initio* calculations [BRO 68, DOC 72]. The outer *ab initio* regions of the [STW 77] curves were scaled to fit smoothly onto the RKR and long-range points. The scaling procedure was analyzed more thoroughly in [STW 82, VER 82]. The upper large $R$ portion of the $X$ state hybrid curve [STW 77] was tested against a new RKR curve which covered the 99% of the well for the $^6$LiH isotopomer [STW 82; VER 82]; the older hybrid curve was in excellent agreement with the new experimental curve.

The Pardo *et al.* [PAR 86, PAR 86A, PAR 86B, PAR 88] hybrid potential energy curves are PMO-RKR-van der Waals curves. A ten-parameter perturbed Morse oscillator (PMO) represents the minimum of the curve (between $R_{0+}$ and $R_{0-}$). The RKR region extends the curve to the uppermost turning points where the adjoining innermost repulsive and outermost attractive regions are represented by an inverse power expansion $+\Sigma C_n/R^n$, where $n = 6, 8, \ldots, 20$, and 22. These $C_n$ constants bear no connection to dispersion coefficients (such as in [STW 77]) and are determined by least-squares fits of the uppermost inner and outer RKR turning points. Hybrid PMO-RKR-van der Waals curves are tabulated for $^7$LiH, $^7$LiD, $^6$LiH and $^6$LiD for both $X$ and $A$ states [PAR 68B].

The hybrid potential energy curve for the $B\ ^1\Pi$ state [WAY 73, ZEM 78B] consists of an isotopically combined RKR well, plus a long-range expansion $-C_6R^{-6} - C_8R^{-8}$ and an exponential upper inner wall. The experiments of [LUH 88] give very good agreement with theoretical results [ZEM 78B, ZEM 78C] which utilized this hybrid curve.

### 2.5. Dissociation Energy

Although Crawford and Jorgensen reported dissociation energies for $X\ ^1\Sigma^+$ and $A\ ^1\Sigma^+$ states of LiH and LiD, the values were quite uncertain (±0.2 eV [CRA 36]). The first precise value for the dissociation energy $D_e$ of the $X$ state of $^7$LiH came from Velasco's observation of predissociation in the $B\ ^1\Pi$ state [VEL 57]. His extrapolation with the limiting curve of dissociation method [HER 50, GAY 68] resulted in precise $T_e$ and $D_e$ values for the $B$ state. From the energy-balance formula $D_e'' = T_e + D_e' - [E(2p\ ^2P^0) - E(2s\ ^2S)]$, where the atomic transition energy (14903.89 cm$^{-1}$ [MOO 71]) was well known, Velasco obtained $D_e = 20{,}289 \pm 2$ cm$^{-1}$ for $^7$LiH in the $X$ state (20,294 ± 8 cm$^{-1}$ for $^7$LiD) [VEL 57]. In similar fashion for the $A$ state, [VEL 57] obtained $D_e = 8{,}683 \pm 2$ cm$^{-1}$ for $^7$LiH (8,687 ± 8 cm$^{-1}$ for $^7$LiD); for the $B$ state he reported $D_e = 284 \pm 8$ cm$^{-1}$ for $^7$LiH (291 ± 16 cm$^{-1}$ for $^7$LiD).

Way and Stwalley [WAY 73] used rotational predissociation data of [VEL 57] and the method of mass-reduced quantum numbers to obtain for $^7$LiH the precise $D_e$ values 20,286.7 ± 0.5 cm$^{-1}$, 8,680.7 ± 0.5 cm$^{-1}$ and 287.9 ± 0.5 cm$^{-1}$ for the $X$, $A$ and $B$ states, respectively. Stwalley *et al.* [STW 74] reexamined the $B$-$X$ data of [VEL 57], performed an analysis like that of [WAY 73], and reported considerably improved precision for the dissociation energies for $^7$LiD. Vidal and Stwalley [VID 82, VID 84] included adiabatic corrections and obtained values for $X$, $A$ and $B$ states for all four isotopic combinations. Chan *et al.* [CHA 86] improved the adiabatically corrected Dunham coefficients of [VID 82] for $X$ and $A$ states; [CHA 86] constants (for $X$ and $A$ states) and [VID 84] constants (for the $B$ state) are used to calculate ZPE's which in turn are used to determine the recommended dissociation energies listed in Table 2.

### 2.6. Electronic Structure Calculations

Early *ab initio* calculations on lithium hydride were usually confined to the ground state and were typically studies of various wave function types (e.g. MO [KAR 59A], VB [KAR 59] or CI [KAR 59, KAR 59A]) and orbital types (e.g. elliptic [BEN 66], STO [CAD 67], GTO [CSI 66] or FSGO [FRO 67]) often restricted to the (approximate) experimental equilibrium distance $R_e$ (3.015 $a_0$). Moreover, many early single configuration calculations used minimal or limited basis sets; see the bibliography in [CAD 67], for example.

The first single configuration calculations at the Hartree-Fock (HF) level are those of Bender and Davidson [BEN 66] and Cade and Huo [CAD 67]. Not all early configuration interaction (CI) calculations resulted in improved binding energies (lower electronic energies) better than these HF limit calculations at $R_e$. However, often the effect on the binding energy of the inclusion of more configurations (CSFs) in the CI calculation was examined and potential energy curves were often computed (e.g. [KAR 59]). Table 13 lists a number of high quality calculations at the HF level or better; particular emphasis is on more recent calculations and those that present electronic structure information beyond just the energy at $R_e$ (e.g. $V(R)$, $\mu(R)$, $D(R)$ functions and spectroscopic constants). Earlier calculations may be located in early compendia [CAD 67, KRA 67, RIC 71, RIC 74].

Table 13 does not include each and every *ab initio* calculation on the structure and properties of lithium hydride. Many references, describing new formalisms or model development using LiH as a test system (frequently along with other molecular systems), are omitted from the table. Some may be noted in Secs. 2.7 and 2.8 or identified separately later in this section. Papers on the analysis of correlation effects in the molecular wave function (by orbital optimization, for example) are excluded from this review.

TABLE 13. High quality calculations of LiH (Hartree Fock or better) normally calculated at $R_e$ ($N$ indicates lowest point, not $R_e$; $E$ indicates experimental $R_e$); $\infty$ means asymptotic energy calculations

| WF Type | Orbital Type | State | $E$(a.u.) | $D_e$(cm$^{-1}$) | $R_e(a_0)$ | Range of $V(R)$ | Spect. Const. | Other Comments | Ref. |
|---|---|---|---|---|---|---|---|---|---|
| VB–CI | Num HF | $X\,^1\Sigma^+$ | | 13,039 | 3.0 | 2.0 – 8.0 | √ | $\mu(R)$ | KAR 59, |
| | | $A\,^1\Sigma^+$ | | 7,992 | 5.0 | 2.0 – 8.0 | √ | $\mu(R)$, $D(R)$, $f$ | KAR 60 |
| MO–CI | Num HF | $X\,^1\Sigma^+$ | | 13,045 | 3.0 | 2.0 – 8.0 | | $\mu(R)$ in figure | KAR 59A |
| | | $A\,^1\Sigma^+$ | | 7,999 | 5.0 | 2.0 – 8.0 | | | |
| CI | elliptic | $a\,^3\Sigma^+$ | | | | 1.0 – 10.0 | | repulsive | TAY 63 |
| MO | elliptic | $X\,^1\Sigma^+$ | −7.98711$^E$ | | 3.015$^E$ | | | | BEN 66 |
| NO–CI | elliptic | $X\,^1\Sigma^+$ | −8.06062$^E$ | 18,100 | 3.015$^E$ | | | $\mu$ | BEN 66 |
| MO | GTO | $X\,^1\Sigma^+$ | −7.984206$^E$ | | 3.02$^E$ | 2.6 – 3.5 | √ | $\mu(R)$ | CSI 66 |
| MO | STO | $X\,^1\Sigma^+$ | −7.987313$^E$ | | 3.015$^E$ | 2.0 – 4.2, $\infty$ | √ | | CAD 67 |
| CI | STO | $X\,^1\Sigma^+$ | −8.0036$^E$ | | 3.015$^E$ | 1.5 – 6.0 | | $\mu(R)$, $f$ | BEN 68 |
| | | $a\,^3\Sigma^+$ | | | | 1.5 – 6.0 | | repulsive; $\mu(R)$; 4 more $^3\Sigma^+$ states reported | |
| | | $A\,^1\Sigma^+$ | −7.8979$^N$ | | 4.5$^N$ | 1.5 – 6.0 | | $\mu(R)$; 4 more $^1\Sigma^+$ states reported | |
| | | $B\,^1\Pi$ | | | | 1.5 – 6.0 | | unbound; $\mu(R)$; 2 more $^1\Pi$ states reported | |
| | | $b\,^3\Pi$ | −7.8666$^N$ | | 4.0$^N$ | 1.5 – 6.0 | | $\mu(R)$; 2 more $^3\Pi$ states reported | |
| | | $^3\Delta$ | −7.7937$^N$ | | 4.0 – 4.5$^N$ | 1.5 – 6.0 | | $\mu(R)$ | |
| | | $^1\Delta$ | −7.7936$^N$ | | 4.0 – 4.5$^N$ | 1.5 – 6.0 | | $\mu(R)$ | |
| CI | elliptic | $X\,^1\Sigma^+$ | −8.0556 | | 3.060 | 1.0 – 10.0 | √ | $\mu(R)$ | BRO 68 |
| | | $A\,^1\Sigma^+$ | −7.9372 | | 4.928 | | √ | $\mu(R)$ | |
| | | $C\,^1\Sigma^+$ | | | 3.70 | | | $\mu(R)$; second min near 10 $a_0$ | |
| | | $^1\Sigma^+$ | | | ~7.0 | | | $\mu(R)$ | |
| GVB | STO | $X\,^1\Sigma^+$ | −8.0173$^E$ | 15,310 | 3.015$^E$ | | | $\mu$ | PAL 69 |
| CI | STO | $X\,^1\Sigma^+$ | −7.989861 | | 3.035 | 1.7 – 9.0 | √ | $G(v)$, $B_v$ values; $\mu$ | SAH 69 |
| MCSCF | STO | $X\,^1\Sigma^+$ | −8.01488$^E$ | | 3.02$^E$ | | | | MUK 70 |
| MCSCF | STO | $X\,^1\Sigma^+$ | −8.021321 | 19,450 | 3.049 | 2.0 – 12.0 | √ | $\Delta G_v$, $B_v$ values; $\mu(R)$,$q$,$Q$, $D_{AX}(R)$ | DOC 72, |
| | | $a\,^3\Sigma^+$ | | | | 2.0 – 12.0 | | repulsive; $\mu(R)$, $D_{ab}(R)$ | DOC 72A |
| | | $A\,^1\Sigma^+$ | −7.903574 | 8,450 | 4.996 | 2.0 – 12.0 | | $\Delta G_v$, $B_v$ values; $\mu(R)$, $q$, $Q$, $D_{AB}(R)$ | |
| | | $B\,^1\Pi$ | −7.7865709 | 137 | 4.688 | 2.0 – 12.0 | | $\Delta G_v$, $B_v$ values; $\mu(R)$, $q$, $Q$, $D_{BX}(R)$ | |
| | | $b\,^3\Pi$ | −7.873358 | 1,820 | 3.693 | 2.0 – 12.0 | | $\Delta G_v$, $B_v$ values; $\mu(R)$, $q$, $Q$ | |
| GVB | STO | $X\,^1\Sigma^+$ | −8.01605$^E$ | | 3.015$^E$ | | | $\mu$, $Q$, $q$; IP(LiH) = 7.60 eV | MEL 72 |
| | | $a\,^3\Sigma^+$ | | | | | | $\mu$, $Q$, $q$; 3 more $^3\Sigma^+$ states reported | |
| | | $A\,^1\Sigma^+$ | −7.89982$^E$ | | 3.015$^E$ | | | $\mu$, $Q$, $q$; 3 more $^1\Sigma^+$ states reported | |
| | | $B\,^1\Pi$ | −7.86165$^E$ | | 3.015$^E$ | | | 2 more $^1\Pi$ states reported | |
| | | $b\,^3\Pi$ | −7.87555$^E$ | | 3.015$^E$ | | | 2 more $^3\Pi$ states reported | |
| MCSCF | STO | $X\,^1\Sigma^+$ | −8.00371 | | 3.10 | 2.0 – 8.0, $\infty$ | √ | $\mu(R)$ | KUP 74 |
| CEPA | GTO | $X\,^1\Sigma^+$ | −8.064705 | 19,970 | 3.015 | 2.2 – 4.8, $\infty$ | √ | $\mu(R)$ | MEY 75 |
| VB–CI | GTO | $X\,^1\Sigma^+$ | | 18,040 | 3.119 | 2.5 – 10.0 | | $V(R)$ in figure only | YAR 76 |
| | | $A\,^1\Sigma^+$ | | 8,099 | 4.89 | 2.5 – 10.0 | | $V(R)$ in figure only | |
| | | $C\,^1\Sigma^+$ | | | | 2.5 – 10.0 | | $V(R)$ in figure only, repulsive | |
| VB–CI | elliptic | $X\,^1\Sigma^+$ | −8.0630 | | 3.015 | | | wf includes interelectronic distance $r_{ij}$ | CLA 77 |
| CI | STO | $X\,^1\Sigma^+$ | −8.023892 | 20,070 | 3.040 | 1.8 – 20.0, $\infty$ | √ | $\Delta G_v$ values | LIU 77 |

TABLE 13. High quality calculations of LiH (Hartree Fock or better) normally calculated at $R_e$ (N indicates lowest point, not $R_e$; E indicates experimental $R_e$); ∞ means asymptotic energy calculations – Continued

| WF Type | Orbital Type | State | $E$(a.u.) | $D_e$(cm$^{-1}$) | $R_e$($a_0$) | Range of $V(R)$ | Spect. Const. | Other Comments | Ref. |
|---|---|---|---|---|---|---|---|---|---|
| GVB | GTO | $X\ ^1\Sigma^+$ | −8.02620 | 20,360 | 3.027 | 1.75 − 20.0 | √ | $\mu(R)$ | GAT 80 |
| | | $a\ ^3\Sigma^+$ | | | | 1.75 − 20.0 | | repulsive, $\mu(R)$ | |
| | | $A\ ^1\Sigma^+$ | −7.88708 | 7,993 | 5.595 | 1.75 − 20.0 | √ | $\mu(R)$, ($D_e$ misprint in paper) | |
| | | $B\ ^1\Pi$ | −7.77787$^N$ | | 14.0$^N$ | 1.75 − 20.0 | | $\mu(R)$ | |
| | | $b\ ^3\Pi$ | −7.807662 | 6,540 | 3.124 | 1.75 − 20.0 | √ | $\mu(R)$ | |
| | | $C\ ^1\Sigma^+$ | −7.77776$^N$ | | 12.0$^N$ | 1.75 − 20.0 | | $\mu(R)$ | |
| UHF–PT2 | GTO | $X\ ^1\Sigma^+$ | −7.9867 | 19,840 | 3.010 | 2.0 − 20.0 | √ | | KLI 80 |
| MCSCF–CI | GTO | $X\ ^1\Sigma^+$ | −8.05428 | 20,000 | 3.015 | 2.0 − 7.365, ∞ | √ | $\mu$, $Q$, $eqQ$; $\Delta G_v$ values; 728 CSFs | JON 81 |
| CI | STO | $X\ ^1\Sigma^+$ | −8.063847$^N$ | 19,972 | 3.0$^N$ | 1.75 − 20.0, ∞ | | $\mu_v$, $\mu(R)$, $D_{AX}(R)$; $G_v$ values; $A_v$ | PAR 81 |
| | | $A\ ^1\Sigma^+$ | −7.944430$^N$ | 9,042 | 4.75$^N$ | 1.75 − 20.0, ∞ | | $\mu_v$, $\mu(R)$, $D_{AB}(R)$; $G_v$ values; $A_v$, $\tau_v$ | |
| | | $B\ ^1\Pi$ | −7.903550$^N$ | 284 | 4.5$^N$ | 1.75 − 20.0, ∞ | | $\mu_v$, $\mu(R)$, $D_{BX}(R)$; $G_v$ values; $A_v$, $\tau_v$ | |
| CI | STO | $A\ ^1\Sigma^+$ | | 8,653 | 4.783 | 1.75 − 25.0 | | $\mu_v$, $\mu(R)$, $\Delta G_v$ values; $A_v$, $\tau_v$ | PAR 81A |
| MCSCF Pseudo-potential | STO | $X\ ^1\Sigma^+$ | | 18,861 | 2.986 | 2.0 − 30.0, ∞ | √ | | STE 81, KAR 78 |
| | | $a\ ^3\Sigma^+$ | | | | 2.0 − 30.0, ∞ | | repulsive | |
| QMC | GTO | $X\ ^1\Sigma^+$ | −8.067 | | 3.015 | | | | REY 82 |
| CASSCF | GTO | $X\ ^1\Sigma^+$ | −8.02065 | 19,600 | 3.044 | 1.915 − 20.0 | √ | $\mu(R)$, $\alpha(R)$ | ROO 82 |
| MBPT | STO | $X\ ^1\Sigma^+$ | −8.0653 | | 3.015 | | | | WIL 82 |
| MRSDCI | GTO | $X\ ^1\Sigma^+$ | −8.06904$^E$ | | 3.015$^E$ | | | $\mu$; 132,000 CSFs | HAN 84 |
| VB–CI | STO | $X\ ^1\Sigma^+$ | | 19,644 | 3.038 | 1.83 − 20.0 | | $\mu(R)$; 188 CSFs | COO 85 |
| QMC | GTO | $X\ ^1\Sigma^+$ | −8.0700$^E$ | 20,200 | 3.015$^E$ | | | $\mu$, $Q$ | BAR 87, LES 90 |
| Pseudo-potential CI | GTO | $X\ ^1\Sigma^+$ | | 19,680 | 3.01 | | √ | | FUE 87 |
| CC | GTO | $X\ ^1\Sigma^+$ | −8.05858 | 19,560 | 3.015 | 2.0 − 10.0, ∞ | √ | | BEN 88 |
| | | $a\ ^5\Sigma^+$ | | | | 2.0 − 10.0, ∞ | | repulsive | |
| | | $A\ ^1\Sigma^+$ | | 8,445 | 4.91 | 2.0 − 10.0, ∞ | √ | | |
| | | $B\ ^1\Pi$ | | 89 | 4.695 | 2.0 − 10.0, ∞ | √ | | |
| | | $b\ ^3\Pi$ | | 1,740 | 3.74 | 2.0 − 10.0, ∞ | √ | | |
| MBPT | | $X\ ^1\Sigma^+$ | | 18,230 | 3.0153 | 2.0 − 10.0 | √ | $V(R)$ in figure only | WAN 89 |
| | | $a\ ^3\Sigma^+$ | | | | 2.0 − 10.0 | | repulsive; $V(R)$ in figure only | |
| | | $A\ ^1\Sigma^+$ | | 8,630 | 4.901 | 2.0 − 10.0 | √ | $V(R)$ in figure only | |
| | | $B\ ^1\Pi$ | | 89 | 4.998 | 2.0 − 10.0 | √ | $V(R)$ in figure only | |
| | | $b\ ^3\Pi$ | | 1,620 | 3.76 | 2.0 − 10.0 | √ | $V(R)$ in figure only | |
| MRCI | | $X\ ^1\Sigma^+$ | −8.0393$^N$ | 19,500 | 3.0$^N$ | 1.0 − 35.0 | | | MEN 90 |
| | | $A\ ^1\Sigma^+$ | −7.9326$^N$ | 8,780 | 4.5$^N$ | 1.0 − 35.0 | | 3 more $^1\Sigma^+$ states reported | |
| | | $B\ ^1\Pi$ | −7.8932$^N$ | | 4.5$^N$ | 1.0 − 35.0 | | 1 more $^1\Pi$ state reported | |
| MCTDHF | GTO | $X\ ^1\Sigma^+$ | | 18,764 | 3.050 | 1.0 − 7.0 | | $\mu(R)$, $D_{AX}(R)$ and $V(R)$ in figure only; $\Delta G_v$ values | SAS 90 |
| | | $A\ ^1\Sigma^+$ | | 8,212 | 4.679 | 1.0 − 7.0 | | $D_{AB}(R)$ and $V(R)$ in figure only; $\Delta G_v$ values | |
| | | $B\ ^1\Pi$ | | 188 | 4.925 | 1.0 − 7.0 | | $D_{BX}(R)$ and $V(R)$ in figure only; $\Delta G_v$ values | |
| Multiref. CCSD | GTO | $X\ ^1\Sigma^+$ | −8.060833$^E$ | | 3.015$^E$ | 2.5 − 15.0 | | | BAL 91 |
| | | $a\ ^3\Sigma^+$ | | | | 2.5 − 15.0 | | repulsive | |
| | | $A\ ^1\Sigma^+$ | −7.942045$^N$ | | | 2.5 − 15.0 | | | |
| | | $B\ ^1\Pi$ | −7.902659$^N$ | | | 2.5 − 15.0 | | | |
| | | $b\ ^3\Pi$ | −7.909690$^N$ | | | 2.5 − 15.0 | | | |

In addition to presenting a chronology of the advancing frontier in improvements and new developments in diatomic molecular electronic structure calculations, entries in the table provide a number of interesting comparisons. For example, there are early single configuration calculations with different basis set types: elliptic [BEN 66] versus Gaussian-type [CSI 66] versus Slater-type orbitals [CAD 67]. Brown and Shull [BRO 68] and Clary and Handy [CLA 77] both used elliptical orbitals, but [CLA 77] explicitly used the interelectronic distance $r_{ij}$ in their Hylleras-type wave function. Another comparison is afforded in the GVB (e.g. [MEL 72]) and MCSCF (e.g. [DOC 72]) procedures, for a variety of electronic states. The comparison of many-body perturbation theory (e.g. [WIL 82]) and comparable CI calculations (e.g. [HAN 84]) is noteworthy. The near equality of very large CI (e.g. [HAN 84]) calculations and newer but nonvariational quantum Monte Carlo [BAR 87, LES 90] calculations is interesting for the ground state case.

Long-range CI in the $^1\Sigma^+$states of LiH has been studied by a number of workers [BAT 56, OLS 71, GRI 74, JAM 76, ADE 77, MEN 90]. Several workers [STA 68, KOU 73, KOU 74, FIG 84, BUS 86] calculated *ab initio* long-range $C_6$, $C_8$ and $C_{10}$ dispersion coefficients for ground state atoms (corresponding to the $X\ ^1\Sigma^+$ and $a\ ^3\Sigma^+$ states); [BUS 86] also determined them for a number of excited states. Semiempirical values of $C_6$, $C_8$ and $C_{10}$ are also available from several sources for ground state atoms [DAL 59, DAL 66, KRA 70, TAN 76, PRO 77] and also the $B\ ^1\Pi$ [WAY 73] and $A\ ^1\Sigma^+$ [STW 77] states.

Long-range exchange corresponding to the potential difference between $X\ ^1\Sigma^+$ and $a\ ^3\Sigma^+$ states has been studied [KNO 69, SHP 79]. Other calculations on $X$ and $A$ state interaction potentials resulted in spin-exchange cross sections for the collision of H and Li [COL 85].

The proton affinity of LiH has been calculated [DIX 88].

All of the above electronic structure calculations were nonrelativistic and also in the Born-Oppenheimer (fixed nuclei) approximation. As noted above in subsection 2.4, there have been a variety of theoretical calculations of the adiabatic corrections to the Born-Oppenheimer approximation [KLE 73, KLE 74, KLE 74A, BUN 77, BIS 83, BIS 83A, BIS 83B, HAD 86, OGI 87, JEN 88]. However, the values tabulated in Table 13 refer to fixed, point nuclei, i.e. infinitely massive $^\infty H^+$ and $^\infty Li^{+3}$. Calculations determining the nonadiabatic coupling function between the $X$ and $a$ states have also been reported [CIM 80].

### 2.7. Radiative and Dipole Properties

Experimental and theoretical dipole moments or dipole moment derivatives have been reported by many workers [HUR 57, NOR 58, WHA 60, WHA 62, LAW 63, BEN 66, PAL 69, ROT 69, SAH 69, MEL 72, LAN 78, BRI 80, CIM 80, DAG 80B, ADA 81, JON 81, BRI 83, BRI 84, HAN 84, BIS 85, ROO 85, MAR 86, BAR 87, SUN 88, RER 91]. Dipole moment functions $\mu(R)$ for the ground state have been determined frequently [KAR 59, JAM 60, KAR 60, CSI 66, DOC 72A, KUP 74, MEY 75, ROO 82, COO 85, KUR 85, VOJ 85, WEI 87, SAS 90]; some workers reported $\mu(R)$ functions for excited states along with the ground state [BEN 68, BRO 68, DOC 72A, GAT 80, PAR 81, PAR 81A]. Dipole moment matrix elements and line strengths have been calculated for the purely vibrational transitions in the $X\ ^1\Sigma^+$ state [DOC 72A, ZEM 80]; Franck-Condon factors for $X$ state vibrational–rotational transitions have also been determined [ZEM 80].

Transition moment functions $D(R)$ have been determined, mostly for $A$–$X$ transitions [KAR 60, DOC 72A, CIM 80, ENN 81, KUR 85, RER 91]; $D(R)$ functions for $B$–$X$ transitions [DOC 72A, KUR 85] and $^3\Pi$–$^3\Sigma^+$ transitions [DOC 72A] have been reported. Using the Docken and Hinze $D(R)$, line strengths for $A$–$X$ transitions have been computed [DOC 72A, KIR 78, ZEM 78], as have individual $A$–$X$ transition moment matrix elements [OPP 74, DOC 75, ZEM 78]; [ZEM 78B] computed $B$–$X$ and $A$–$B$ transition moment matrix elements with the [DOC 72A] $D(R)$ functions. Franck-Condon factors [HAL 67, OPP 74, ZEM 78, PAR 86] and $R$-centroids [HAL 67, DOC 75, ENN 81] have been reported for $A$–$X$ transitions; [ZEM 78B] computed Franck-Condon factors for $B$–$X$ and $A$–$B$ transitions.

Radiative lifetimes have been reported for the $A\ ^1\Sigma^+$ state [DAG 76, WIN 76, ZEM 78A, KUR 85, VON 87, WEI 87] and $B\ ^1\Pi$ state [ZEM 78C]. Zemke and Stwalley reported Einstein $A$ coefficients for the $A$ state [ZEM 78, ZEM 78A] and $B$ state [ZEM 78B]. Nonradiative decay of the $A\ ^1\Sigma^+$ state through the ionic-covalent curve crossing is expected to be negligible (see Sec. 2.8).

Oscillator strengths for transitions from the ground state to various excited $^1\Sigma^+$ and $^1\Pi$ states have been reported [KAR 60, BEN 68, STE 75, WAT 76, SAS 90].

Cashion [CAS 64] presented a comparison of $X\ ^1\Sigma^+$ vibration-rotation interaction (Herman-Wallis) factors and transition probabilities from relative line intensities.

### 2.8. Other Properties

Other properties of LiH which have been studied are polarizabilities [ADA 69, ARR 70A, WAT 76, DOD 77, GRE 77, HAL 77, KAR 82, LAZ 82, BIS 85, MAL 85, MAR 86A, SAS 90, RER 91], quadrupole moments [ROT 69, ARR 70, DOC 72A, MEL 72, DOC 74, FRE 75, ADA 81, SUN 84, BIS 85, ROO 85, MAR 86, SUN 88, URB 90], electric field gradients [DOC 72A, MEL 72, DOC 74, LAZ 82, PIE 84, HUB 85, SUN 85, NAZ 89, PAI 90, URB 90], nuclear quadrupole coupling constants [GUO 87, PAI 90], rotational magnetic moments [LAW 63, DOC 74, FRE 75], and magnetic susceptibilities [WHA 62, KAR 63, STE 63, DEL 64, ARR 70A, FRE 75, KEI 79, HOE 80, DAB 81].

It is clear that nonradiative decay of the $A\ ^1\Sigma^+$ state can potentially occur because of the change in electronic configuration with internuclear distance (ionic-covalent

curve crossing). [ZEM 78A] estimated a $10^{-6}$ second non-radiative lifetime for levels with a classical turning point beyond the avoided crossing distance, $R_c$ = 3.8570 Å, i.e., $v' \gtrsim 5$ (see Sec. 3). Recent approximate quantitative calculations confirm this estimate [TIL 91].

Collisional ionization cross sections ($Li + H^* \rightarrow Li^* + H^+ + e^-$) have been determined [LOD 69]. Studies of ion-ion recombination ($H^- + Li^+ \rightarrow H^+ + Li^*$) have been reported [BAT 56, OLS 71, GRI 74, JAN 76, JAN 78, MEN 90]. The reverse reaction (ion-pair formation) has been studied experimentally [DYA 72] and theoretically [JAN 78].

### 2.9. Positive Ions

Although $LiH^+$ has never been observed experimentally (except in a mass spectrometer [IHL 75]), a wide variety of collisional experiments and cross section calculations (reviewed in [ALV 81, MOR 85]) which probe the $LiH^+$ potential energy curves has been reported: for the charge transfer reaction $Li + H^+ \rightarrow Li^+ + H(nl)$ [ILI 67, DYA 68, DYA 69, GRU 69, GRU 70, KUB 81, KIM 82, OLS 82, ALL 83, FRI 83, SAT 83, ERM 84, VAR 84, GIE 91] and the electron loss reaction $Li^+ + H \rightarrow Li^{2+} + H^-$ [PEA 89, SHA 91]. Theoretical calculations on the structure of $LiH^+$ are numerous; see Table 14.

TABLE 14. High quality calculations of $LiH^+$ normally calculated at $R_e$ ($v$ indicates at neutral ground state $R_e$; N indicates lowest point, not $R_e$)

| WF Type | Orbital Type | State | $E$(a.u.) | $D_e$(cm$^{-1}$) | $R_e(a_0)$ | Range of $V(R)$ | Spect. Const. | Other Comments | Ref. |
|---|---|---|---|---|---|---|---|---|---|
| VB | STO | $X\,^2\Sigma^+$ | −7.6975$^v$ | | 3.014$^v$ | 0.5 − 6.0 | | $\zeta$ − optimized at each $R$ | PLA 59 |
| MO | STO | $X\,^2\Sigma^+$ | −7.68392$^N$ | | 3.90$^N$ | 2.0 − 7.0 | √ | min basis | FRA 61 |
| VB | STO/ elliptic | $X\,^2\Sigma^+$ | −7.780848 | >310 <1,210 | 4.25 | | | $IP$(LiH) ≥ 7.81 eV | BRO 64 |
| MO | STO | $X\,^2\Sigma^+$ | −7.72943$^v$ | | 3.015$^v$ | | | Hartree-Fock limit, vert $IP$(LiH) = 7.02 eV | CAD 67 |
| VB–CI | elliptic | $X\,^2\Sigma^+$ | −7.758855 | | 3.736 | | | μ | LIN 69 |
| UHF | GTO | $X\,^2\Sigma^+$ | −7.7250231$^N$ | | 3.3$^N$ | 2.1 − 3.5 | | hyperfine coupling constants | CLA 70 |
| Model Potential | GTO | $X\,^2\Sigma^+$ | | 730 | 4.5 | | | one-electron model | SCH 72 |
| FSGO | GTO | $X\,^2\Sigma^+$ | −7.738318 | 1,960 | 3.370 | | | 2 CSFs | BLU 74 |
| Effective Potential | SDO | $X\,^2\Sigma^+$ | −7.67498 | | 3.339 | 2.0 − 4.0 | | μ | AUB 75 |
| VB–CI | GTO | $X\,^2\Sigma^+$ | | 830 | 4.321 | 2.5 − 10 | | $V(R)$ in figure only; vert $IP$(LiH) = 6.7 eV | YAR 76 |
| | | $A\,^2\Sigma^+$ | | | | 2.5 − 10 | | $V(R)$ in figure only | |
| | | $C\,^2\Pi$ | | | | 2.5 − 10 | | $V(R)$ in figure only, unbound | |
| PNO–CI | GTO | $X\,^2\Sigma^+$ | −7.782310 | | 4.14 | | √ | | ROS 77 |
| CEPA | GTO | $X\,^2\Sigma^+$ | −7.782314 | 1,050 | 4.14 | | √ | proton affinity | ROS 77 |
| CI | STO | $X\,^2\Sigma^+$ | −7.7569 | 1,050 | 4.23 | 3.5 − 6.5 | | nuclear spin densities, μ | TOR 78 |
| | | $C\,^2\Pi$ | | | | | | unbound | |
| Pseudo-potential | GTO | $X\,^2\Sigma^+$ | | 1,130 | 4.12 | | √ | with core polarization | FUE 82 |
| Pseudo-potential | STO | $A\,^2\Sigma^+$ | | 3,950 | 7.47 | 2.0 − 25 | | $V(R)$ in figure only | KIM 82 |
| | | $B\,^2\Sigma^+$ | | | | 2.0 − 25 | | $V(R)$ in figure only | |
| | | $C\,^2\Pi$ | | | | 2.0 − 25 | | $V(R)$ in figure only | |
| | | $D\,^2\Pi$ | | | | 2.0 − 25 | | $V(R)$ in figure only | |
| | | $E\,^2\Sigma^+$ | | | | 2.0 − 25 | | $V(R)$ in figure only, unbound | |
| | | $F\,^2\Sigma^+$ | | | | 2.0 − 25 | | $V(R)$ in figure only, unbound | |
| Pseudo-potential | STO | $A\,^2\Sigma^+$ | | 3,900 | 7.47 | 2.0 − 30 | | $V(R)$ in figure only | ALL 83 |
| | | $B\,^2\Sigma^+$ | | | | 2.0 − 30 | | $V(R)$ in figure only | |
| | | $C\,^2\Pi$ | | | | 2.0 − 30 | | $V(R)$ in figure only | |
| | | $D\,^2\Pi$ | | | | 2.0 − 30 | | $V(R)$ in figure only | |
| | | $E\,^2\Sigma^+$ | | | | 2.0 − 30 | | $V(R)$ in figure only, unbound | |
| | | $F\,^2\Sigma^+$ | | | | 2.0 − 30 | | $V(R)$ in figure only, unbound | |

TABLE 14. High quality calculations of $LiH^+$ normally calculated at $R_e$ ($v$ indicates at neutral ground state $R_e$; N indicates lowest point, not $R_e$) – Continued

| WF Type | Orbital Type | State | $E$(a.u.) | $D_e(cm^{-1})$ | $R_e(a_0)$ | Range of $V(R)$ | Spect. Const. | Other Comments | Ref. |
|---|---|---|---|---|---|---|---|---|---|
| Model potential | TDO | $X\,^2\Sigma^+$ | | 1,050 | 4.08 | 2.0 – 20 | | $V(R)$ in table and figure | ALI 85 |
| | | $A\,^2\Sigma^+$ | | 4,030 | 7.35 | 2.0 – 20 | | $V(R)$ in table and figure | |
| | | $B\,^2\Sigma^+$ | | 4,270 | 7.11 | 2.0 – 20 | | $V(R)$ in table and figure | |
| | | $C\,^2\Pi$ | | | | 2.0 – 20 | | $V(R)$ in table and figure | |
| | | $D\,^2\Pi$ | | | | 2.0 – 20 | | $V(R)$ in table and figure; 12 more $^2\Pi$ states reported | |
| | | $E\,^2\Sigma^+$ | | 5,400 | 11.6 | 2.0 – 20 | | $V(R)$ in table and figure | |
| | | $F\,^2\Sigma^+$ | | | | 2.0 – 20 | | $V(R)$ in table and figure; 15 more $^2\Sigma^+$ states reported | |
| | | $^2\Delta$ | | | | 2.0 – 20 | | $V(R)$ in table and figure; 13 more $^2\Delta$ states reported | |
| SCF | GTO | $X\,^2\Sigma^+$ | −7.74062 | | 4.196 | | | | CAR 86 |
| CI | GTO | $X\,^2\Sigma^+$ | −7.74112 | | 4.25 | | | single-excitation CI; $\mu$, nuclear spin densities | DYE 86 |
| One-electron model potential | | $C\,^2\Pi$ | $-0.35082^N$ | | $4.0^N$ | 4, 8, 20 | | five more excited $^2\Pi$ states | JOU 88 |
| | | $^2\Delta$ | $-0.1944^N$ | | $4.0^N$ | 4, 8, 20 | | four more excited $^2\Delta$ states | |
| MRSDCI | GTO | $X\,^2\Sigma^+$ | −7.77619 | 1,070 | 4.149 | 2.0 – 40 | | $q$ for all $R$, $eqQ$ for all isotopomers, $V(R)$ in table and figure | VOJ 90 |
| | | $A\,^2\Sigma^+$ | −7.48416 | 3,330 | 7.27 | 2.0 – 40 | | $q$ for all $R$, $eqQ$ for all isotopomers, $V(R)$ in table and figure | |
| | | $B\,^2\Sigma^+$ | $-7.40700^N$ | 1,370 | $10.5^N$ | 2.0 – 40 | | $q$ for all $R$, $eqQ$ for all isotopomers, $V(R)$ in table and figure | |
| CI | GTO | $X\,^2\Sigma^+$ | | | 4.18 | 2.0 – 7.25 | √ | $V(R)$ in figure only; $G_v$ value; *UV* photoelectron spectrum simulation | GRA 92 |

With respect to the mass spectroscopic study of Ihle and Wu [IHL 75], they determined an experimental ionization potential for $^7LiD$ of 7.7 ± 0.1 eV = 62100 ± 800 $cm^{-1}$. This implies a $D_0(^7LiD^+) = D_0(^7LiD)$[CHA 86] + $IP(^7Li)$[MOO 71] $- IP(^7LiD)$ = 1150 ± 800 $cm^{-1}$. This is in reasonable agreement with the various theoretical calculations of $D_e(LiH^+)$.

Studies on the two-electron "quasimolecule" $LiH^{2+}$ include experiments and calculations for the lithium charge transfer reactions $Li^+ + H^+ \rightarrow Li^{2+} + H(nl)$ [SEW 80, REI 86] and $Li^{2+} + H \rightarrow (Li^+)^* + H^+$ [ERR 85, ERR 85A]. Since the ground state potential energy curve is purely repulsive, there are of course no bound vibrational-rotational levels in the ground electronic state. Theoretical calculations on $LiH^{2+}$ predicted the $^1\Pi$ and $^3\Pi$ states to also be unbound [COL 74]. Calculations involving the one-electron quasimolecule $LiH^{3+}$ include the charge transfer reaction $Li^{3+} + H \rightarrow (Li^{2+})^* + H^+$ [MAN 81, BRA 82, CAS 84, ERR 84, HO 85].

## 2.10. Negative Ions

While the $LiH^-$ ion has not been directly studied experimentally, there are several collisional experiments (reviewed in [ALV 81, MOR 85]) which probe the $LiH^-$ potential energy curves by the charge transfer reaction $Li + H^- \rightarrow Li^- + H$ [DYA 69, AND 80]. A number of theoretical electronic structure calculations have been reported; see Table 15.

Acharya *et al.* [ACH 84] calculate electron detachment rates for the reaction $LiH^-(v) + h\nu \rightarrow LiH(v') + e^-$. Collins *et al.* [COL 80] perform calculations on electron-LiH collisions in electron scattering studies.

## 2.11. Other Comments

Various models for potential energy curves were proposed to reproduce observed spectroscopic constants [VAR 63, KUL 79, PRA 79, RAY 79, CHO 81, KAU 83, PAR 86A, REQ 87, VAR 88]. A modified Rittner model of the ionic adiabatic potential was constructed [YAN 82].

Based on potential energy curves and spectroscopic constants for the various isotopomers, thermodynamic functions at various temperatures have been calculated [STE 40, CHA 83]. Transport coefficients of gaseous LiH for $X\,^1\Sigma^+$ and $a\,^3\Sigma^+$ states have been determined [KRU 63]. Isotopic partition function ratios [HOU 80] and equilibrium constants [CHA 83] for isotopic variance of the gaseous reaction $Li_2 + H_2 = 2LiH$ have been reported. The bulk properties of crystalline LiH have been calculated [PEA 84].

TABLE 15. High quality calculations of $LiH^-$ normally calculated at $R_e$ ($v$ indicates at neutral ground state $R_e$); $\infty$ means asymptotic energy calculation

| WF Type | Orbital Type | State | $E$(a.u.) | $D_e(cm^{-1})$ | $R_e(a_0)$ | Range of $V(R)$ | Spect. Const. | Other Comments | Ref. |
|---|---|---|---|---|---|---|---|---|---|
| SCF-MO | STO | $X\,^2\Sigma^+$ | −7.96644 | | 3.350 | | | vert $EA$(LiH) = −0.17 eV; ad $EA$(LiH) = −0.11 eV | SEL 75 |
| EOM | STO | $X\,^2\Sigma^+$ | | 15,650 | 3.2 | | | vert $EA$(LiH) = 0.30 eV | JOR 76, GRI 75 |
| CI | STO | $X\,^2\Sigma^+$ | −8.035586 | 16,647 | 3.186 | 1.8 − 20, $\infty$ | √ | $V(R)$ in table and figure; ad $EA$(LiH) = 0.32 eV; $\Delta G_v$ values | LIU 77 |
| HF | GTO | $X\,^2\Sigma^+$ | −7.9877 | | | | | vert $EA$(LiH) = 0.23 eV | JOR 78 |
| PNO-CI | GTO | $X\,^2\Sigma^+$ | −8.07371 | 16,050 | 3.15 | | √ | | ROS 78 |
| CEPA | GTO | $X\,^2\Sigma^+$ | −8.07535 | 16,370 | 3.16 | | √ | ad $EA$(LiH) = 0.26 eV | ROS 78 |
| MCSCF Pseudo-potential | STO | $X\,^2\Sigma^+$ | | 15,146 | 3.21 | 2.0 − 30, $\infty$ | √ | $V(R)$ in table and figure; ad $EA$(LiH) = 0.293 eV | STE 81, KAR 78 |
| Num HF | STO | $A\,^2\Sigma^+$ | | 19 | 3.015[v] | | | $\mu$ | MCC 81 |
| Pseudo-potential | | $X\,^2\Sigma^+$ | | >2,580 | | | | $\mu$ | GAR 82, GAR 79 |
| | | $A\,^2\Sigma^+$ | | >21 | | | | | |
| HF | STO | $X\,^2\Sigma^+$ | −7.995142[v] | | 3.015[v] | | | ad $EA$(LiH) = 0.21 eV | ADA 83 |
| | | $A\,^2\Sigma^+$ | −7.987403[v] | | 3.015[v] | | | | |
| Num MCSCF | STO | $A\,^2\Sigma^+$ | | 21[v] | 3.015[v] | | | $\mu$ | ADA 84 |
| Num HF | | $X\,^2\Sigma^+$ | −7.99643[v] | | 3.015[v] | | | vert $EA$(LiH) = 0.25 eV | ADA 85 |
| Num MBPT2 | | $X\,^2\Sigma^+$ | −8.06604[v] | | 3.015[v] | | | vert $EA$(LiH) = 0.28 eV | ADA 85 |
| Num CCSD | | $X\,^2\Sigma^+$ | −8.07866[v] | | 3.015[v] | | | vert $EA$(LiH) = 0.29 eV | ADA 85 |
| | | $A\,^2\Sigma^+$ | −8.06796[v] | | 3.015[v] | | | | |
| Spin-coupled VB | GTO | $X\,^2\Sigma^+$ | | | 3.21 | 2.0 − 10.0 | √ | $V(R)$ in figure only ad $EA$(LiH) = 0.24 eV | FOR 89 |

## 3. Discussion and Conclusions

Although spectroscopic studies on lithium hydride have been performed on many vibrational levels in the potential well (Subsecs. 2.1 and 2.2), experimental studies are needed for missing higher levels of several hydride and deuteride isotopomers. Moreover, there is a complete lack of data on the tritides; such data are very much needed to extend the values for the molecular constants listed in Table 2 and thus the adequacy of the Born-Oppenheimer breakdown approach used.

Further experimental study on the $A$–$X$ bands is needed to experimentally characterize $A \rightarrow X$ bound-continuum emission. Zemke *et al.* [ZEM 78, ZEM 78A] predicted very significant bound-free emission for all $v' > 8$ levels of the $A$ state. Table 16 compares their calculations of bound-free Einstein $A$ coefficients: (i) $A_{v'}$(bound-free) $= (7.2356 \times 10^{-6}) \times |D(R_{v'+})|^2 \; q_{v',\text{continuum}} \; \nu^3_{v',\text{continuum}}$, where $D(R_{v'+})$ is the dipole strength function at the outer classical turning point of level $v'$, the Franck-Condon factor $q_{v',\text{continuum}} = 1 - \sum_{v''} q_{v'v''}$, and $\nu_{v',\text{continuum}}$ is the transition frequency between the level $v'$ and the $X$ state asymptote [ZEM 78A]; (ii) $A_{v'}$(bound-free) $= \int (dA_{v'k''}/dv)dv$, where $A_{v'k''} = 7.2356 \times 10^{-6} \nu^3 |\langle \Psi_{v'} | D(R) | \Psi_{k''} \rangle|^2$ and $\nu$ is the transition frequency between the level $v'$ and the continuum states of energy $E_{k''} = \hbar^2 k''^2/2\mu$) [ZEM 81].

TABLE 16. Bound-free emission in $^7$LiH from $A\,^1\Sigma^+(v',J')$ to $X\,^1\Sigma^+(k'',J'')$

| | Einstein $A_{v'}$(bound→free) coefficients ($10^6 s^{-1}$)[a] | |
|---|---|---|
| $v'$ | from bound-bound calculation [ZEM 78A] | from bound-free calculation [ZEM 79] |
| 23 | 26.3 | 21.1 |
| 24 | 27.8 | 23.0 |
| 25 | 27.8 | 24.4 |
| 26 | 15.8 | 15.0 |

[a] $J' = J'' = 0$

When actual bound-free calculations are not readily available, the comparison in Table 16 shows that a reasonable approximation can be obtained from bound-bound calculations (typically within about 20%). However, further experimental and theoretical investigations are needed to quantitatively characterize the $A \rightarrow X$ continua.

Bound-free emission has been examined only in a cursory fashion for $B \rightarrow X$ transitions in $^7$LiH; [ZEM 78B] calculated Franck-Condon factors $q_{v'v''}$ for all transitions and concluded that bound-free emission occurs, but only from the $v' = 2$ level. Specifically $\sum_{v''=0}^{23} q_{v'=2,v''} = 0.87$ while $\sum_{v''=0}^{23} q_{v',v''} = 1.00$ for both $v' = 0$ and 1 levels [ZEM 78B].

With regard to absorption, the reported continuum in the $B \leftarrow X$ band [VEL 57, VEL 74] has not been studied closely. Based on the Franck-Condon factor calculations of [ZEM 78B], absorption from the $X$ state is primarily into the continuum of the $B$ state: from levels $v'' = 0$, 9, 18 and 23, 99%, 90%, 89% and 52% of the absorption, respectively, is into the $B$ state continuum. Clearly $B \leftarrow X$ bound-free absorption and $B \rightarrow X$ bound-free emission experimental investigations are needed. In addition, precise measurements of the $^6$LiH and $^6$LiD $B$–$X$ bands would be helpful in determining the Li terms in the adiabatic corrections for $D_e$ and $T_e$.

The dominant Dunham coefficients (spectroscopic constants) for the $X\,^1\Sigma^+$ state have remained remarkably unchanged since the pioneering work of Crawford and Jorgensen in 1935 [CRA 35, CRA 35A]; see Table 4. However, the set of very precise constants based on the low-lying levels [MAK 90] does differ slightly from those which were based on a larger data field including higher vibrational-rotational levels [CHA 86]. Adiabatically corrected coefficients for $^7$LiH, $^7$LiD, $^6$LiH and $^6$LiD isotopomers for the $X\,^1\Sigma^+$, $A\,^1\Sigma^+$ and $B\,^1\Pi$ states have been determined (Tables 5–7). No constants have been determined experimentally for the tritides.

In examining the spectroscopic constants of the various isotopomers, several groups [e.g. VID 82, YAM 88, MAK 90] have been able to determine with increased precision the adiabatic corrections to the fundamental zero-order Dunham-type coefficients (Table 17). The spectroscopic constants in the limit of infinite nuclear masses (i.e. $^\infty$Li$^\infty$H) can then be determined simply from the extrapolated values of $Y_{ij}^{(0)}$. Unfortunately, only for $Y_{10}^{(0)}$ ($\approx \omega_e$) and $Y_{01}^{(0)}$ ($\approx B_e$) can the adiabatic Li term be determined in addition to the adiabatic H term. Nevertheless, these $Y_{ij}^{(0)}$ values are the appropriate quantities to compare with nonrelativistic, fixed point nuclei electronic structure calculations.

TABLE 17. Selected Born-Oppenheimer Dunham-type coefficients $Y_{ij}^{(0)}$ ($cm^{-1}$) and their adiabatic corrections ($cm^{-1}$) for the ground $X\,^1\Sigma^+$ state of LiH, scaled to a reduced mass $\mu = 1$ amu. Lines 1, 2 and 3 correspond to results primarily from electronic spectroscopy [VID 82], and infrared ro-vibrational spectroscopy [YAM 88] and [MAK 90], respectively. Line 4 values in brackets are an alternate fit in [MAK 90].

| | | $M_n Y_{ij}^{(1)}$ | |
|---|---|---|---|
| $(i,j)$ | $Y_{ij}^{(0)}$ | N=H | N=Li |
| (1,0) | 1319.78880(742) | −0.44183(366) | – |
| | 1319.9153(41) | −0.5499(31) | −0.0912(239) |
| | 1319.94875(267) | −0.5226(151) | −0.12832(926) |
| | [1319.98677(1132)] | [−0.5405(256)] | [−0.1186(482)] |
| (2,0) | −20.34850(405) | – | – |
| | −20.3889(14) | 0.0160(12) | – |
| | −20.43187(212) | 0.05357(429) | – |
| (0,1) | 6.6264668(687) | −0.004566(132) | −0.0004216(141) |
| | 6.6270748(27) | −0.0057001(69) | −0.0004279(145) |
| | 6.62710473(923) | −0.0056837(405) | −0.00042615(5460) |
| | [6.6271528(473)] | [−0.0057375(144)] | [−0.0004959(2912)] |
| (1,1) | −0.1788157(1158) | – | – |
| | −0.1790128(85) | 0.0000959(89) | – |
| | −0.17914252(691) | 0.0000747(40) | – |
| (0,2) | −0.000667731(233) | – | – |
| | −0.00066706(25) | $-6.77(344)\times 10^{-11}$ | – |
| | −0.0006681488(690) | $1.257(194)\times 10^{-9}$ | – |

The $Y_{01}^{(0)}$ values yield $R_e^{BO}$ values as well; for the recommended $Y_{01}^{(0)}$ value of [MAK 90], one obtains $R_e^{BO} = 1.5949107(11)$ Å, in excellent agreement with the early microwave work (1.59490(2) Å of [PEA 69] and 1.5949132(6) Å [PLU 84, COX 92]). This distance, equivalent to 3.0139442(21) $a_0$ is the equilibrium internuclear distance at which high quality *ab initio* calculations should be carried out (not the approximate value of 3.015 $a_0$ used since the early calculations of Bender and Davidson [BEN 66]).

If one adds the asymptotic binding energy for nonrelativistic, infinite mass, point nuclei (Table 22) to the infinite mass $D_e$ value, one calculates $R_e$ of $^\infty$Li$^\infty$H at 3.0139442 $a_0$, which corresponds to a total binding energy of 1750981.185 + 20299.3 $cm^{-1}$ = 1771280.485 $cm^{-1}$ = 8.070547715 a.u. This slightly exceeds the best *ab initio* values 8.06904 a.u. [HAN 84] and 8.0700 a.u. [BAR 87, LES 90], each calculated at 3.015 $a_0$. The latter value is smaller by only ~120 $cm^{-1}$.

A variety of potential energy curves have been reported for $X$, $A$ and $B$ states, which include Born-Oppenheimer level RKR curves as well as hybrid curves that range over all internuclear distances. Adiabatically corrected IPA curves for these three electronic states for all isotopomers of the hydrides and deuterides are listed

in Tables 8–12. Precise dissociation energies ($D_e$ and $D_0$) and electronic energies $T_e$ have been determined for the hydrides and deuterides; estimates for the tritides and the infinite mass isotopomers are also available, based on values for the hydrides and deuterides (see Table 2). Again, the constants $T_e$ and $D_e$ can be extrapolated to infinite nuclear mass ($1/m \rightarrow 0$), as given in Sec. 1.

The $A\ ^1\Sigma^+$-$X\ ^1\Sigma^+$ ionic-covalent curve crossing in the alkali hydrides has a long history [MUL 36]. We will not discuss this here in detail; the interested reader is referred to [YAN 82] for further discussion. However, we feel it useful to list for $^7$LiH the nominal crossing distance, $R_c$ = 3.8570 Å, the $X\ ^1\Sigma^+$ and $A\ ^1\Sigma^+$ state potentials at $R_c$ (18637.2 cm$^{-1}$ and 1730.8 cm$^{-1}$, respectively, with respect to $V(R_e)$; and −39054.6 cm$^{-1}$ and −29451.2 cm$^{-1}$, respectively, with respect to $^7Li^+ + H^-$), the first derivatives of the potentials at $R_c$ (3137.0 cm$^{-1}$/Å for both states) and the second derivatives at $R_c$ (−5273.2 cm$^{-1}$/Å$^2$ and 2380.0 cm$^{-1}$/Å$^2$, respectively) all of which are obtained from the recommended potentials in this review, in analogy with those given for the heavier alkali hydrides in Table 6.2 of [STW 91]. It should be noted that the changes from earlier results, e.g. from the corresponding experimental values in [YAN 82], are significant. Note that the analysis involves simply finding the two-state "crossing" internuclear distance, $R_c$, which corresponds to the minimum splitting between the $X$ and $A$ potential energy curves, and thus occurs when the slopes of the two curves are identical:

$$\left.\frac{dV_X(R)}{dR}\right|_{R_c} = \left.\frac{dV_A(R)}{dR}\right|_{R_c} .$$

The potential energy in each state is reported not only with respect to $V(R_e)$, but also with respect to the ion pair asymptote, i.e. the asymptote $M^+ + H^-$, calculated using the $D_e$ values in Table 2, the lithium atomic ionization potential (43487.150(5) cm$^{-1}$ from [JOH 59], rather than the less accurate 43487.19 cm$^{-1}$ from [MOO 71]) and the electron affinity of the hydrogen atom (6083.10 cm$^{-1}$ [HOT 85]). The potential energy curves used are the IPA potentials recommended above.

The ionic-covalent crossing is an example of potentially severe breakdown of the Born-Oppenheimer approximation. Nevertheless, LiH results (e.g. [CHA 86]), including non-negligible Born-Oppenheimer breakdown terms in adiabatic potential energy curves, support a purely adiabatic approximation even for $X\ ^1\Sigma^+$ and $A\ ^1\Sigma^+$ levels with significant vibrational amplitude in the region of the ionic-covalent crossing. However, fully nonadiabatic calculations might reveal observable nonadiabatic processes such as electronic predissociation

$$LiH(A\ ^1\Sigma^+, v, J) \rightarrow Li + H .$$

No experimental evidence exists for bands among the $a\ ^3\Sigma^+$, $b\ ^3\Pi$ and $c\ ^3\Sigma^+$ states which (like the $X$, $A$ and $B$ states) correlate with Li + H, Li($2p$) + H and Li($2p$) + H, respectively. Indeed, there are apparently no high quality calculations of the $c\ ^3\Sigma^+$ state, which is presumably very weakly bound with a large $R_e$ value.

No experimental evidence exists for perturbations in LiH spectra. In principle, the vibrational levels of $A\ ^1\Sigma^+$ and $B\ ^1\Pi$ states above the $B$ state minimum could heterogeneously perturb each other. In particular, for $^7$LiH, the unobserved but predicted $A\ ^1\Sigma^+$ vibrational levels $v_A$ = 25 and 26 [STW 77] are in the energy range of the $B\ ^1\Pi$ vibrational levels $v_B$ = 0, 1 and 2. Moreover, the Franck-Condon factors for both $v_A$ levels with $v_B$ = 2 are large, so that such perturbations should occur.

In addition, singlet-triplet perturbations could potentially occur. For example, the $a\ ^3\Sigma^+$ state should be weakly bound at large internuclear distance because of van der Waals attraction (note, however, that all calculated $a\ ^3\Sigma^+$ potential curves in Table 13 are purely repulsive). The levels of this $a^3\Sigma^+$ state may interact with the highest $X\ ^1\Sigma^+$ levels ($v_X$ = 23 and possibly 22 [STW 77]). Likewise weak perturbations may occur between levels of the $b\ ^3\Pi$ and $c^3\Sigma^+$ levels and the $B\ ^1\Pi$ and higher $c^3\Sigma^+$ levels. The possibility that the $X\ ^1\Sigma^+$ continuum predissociates the $A\ ^1\Sigma^+$ state has been estimated [ZEM 78B] to occur with a lifetime of $\sim 10^{-6}$ *s*, much longer than and thus negligible compared to the radiative lifetimes of $\sim 30$ *ns* [ZEM 78B].

The absence of any experimental reports on high-lying electronic states (above the $X$, $A$ and $B$ states) is noteworthy. The only source of information on such electronic excited states is from *ab initio* electronic structure calculations, which have identified and characterized quantitatively many unobserved excited states. Electronic structure calculations have also provided valuable radiative and dipole information for the experimentalists: dipole moment function and matrix elements, transition moment functions and line strengths, and radiative transition probabilities and radiative lifetimes, to name a few. Further experimental studies on the excited states of lithium hydride isotopomers appears to be an area with many exciting research opportunities.

Note in particular that the $LiH^+$ ion is weakly bound, with theoretical $D_e$ values in Table 14 in the range 310–1960 cm$^{-1}$ seemingly converging to ~1100 cm$^{-1}$. Thus, the Rydberg states of LiH will also be weakly bound. Taking the $B\ ^1\Pi$ state as the lowest member of the $^1\Pi$ Rydberg series, it seems that the $2p\pi$ Rydberg orbital is significantly antibonding, with $D_e$(LiH B)$\ll$ $D_e$($LiH^+$ $X$). The $X$ and $A$ states have significant ion pair character and it is not appropriate to consider them as Rydberg. It would be useful to estimate the properties of Rydberg states based on a high quality theoretical calculation of the $LiH^+$ $X\ ^2\Sigma^+$ ground state potential energy curve.

The mass spectroscopic studies of Ihle and Wu [IHL 75] have been discussed in Subsecs. 2.5 and 2.9, where their relatively uncertain results are close to more accurate spectroscopic (2.5) or theoretical (2.9) results. However, one assumption used by [IHL 75] needs to be questioned: that electron impact ionization of LiH leads

exclusively to $LiH^+$. In fact the $X\,^2\Sigma^+$ state of $LiH^+$ is weakly bound and so

$$e^- + LiH \rightarrow Li^+ + H + 2e^-$$

should actually be more probable than

$$e^- + LiH \rightarrow LiH^+ + 2e^-$$

Franck-Condon factor calculations (with $J'' = J' = 0$) [WHA 92] indicate electron-impact ionization or photoionization of $LiH(v'' = 0, 1$ and $2)$ should produce $LiH^+$ (all bound $v'$) with small probabilities (11%, 25% and 29%, respectively), and thus produce $Li^+ + H$ with high probabilities (89%, 75% and 71%, respectively). A similar recent calculation [GRA 92] for $v'' = 0$ but $J''$ variable, finds 8%/92% for $LiH^+/(Li^+ + H)$ for $J'' = 0$ (in good agreement with [WHA 92]), but 2%/98% for $J'' = 10$ and 0%/100% for $J'' = 15$! Thus, one expects not only that the $LiH^+$ mass spectroscopic signal will significantly *underestimate* the true LiH concentration, but also that the amount of underestimation will be significantly temperature dependent. Thus the $D_0(^7LiD)$ value of [IHL 75] should be low; in fact, as discussed in Sec. 2.5, it is slightly high. The reason for this is not known.

## 4. Acknowledgments

The review presented here was aided by literally hundreds of discussions/correspondences with scientific colleagues over the last decade and a half. We particularly wish to thank: J. T. Bahns, C. F. Bender, D. M. Bishop, M. Brieger, Y. C. Chan, M. Chase, L. Covick, J. A. Coxon, P. J. Dagdigian, G. W. Drake, G. Ennen, D. R. Harding, D. R. Herschbach, J. Hinze, E. Hirota, J. R. Hiskes, K. P. Huber, F. Jenč, K. D. Jordan, A. M. Karo, K. Kirby, P. D. Kleiber, S. R. Langhoff, W. A. Lester, K. C. Li, W. T. Luh, A. M. Lyyra, A. G. Maki, W. A. Martin, W. J. Meath, L. A. Melton, J. F. Ogilvie, F. B. Orth, C. Ottinger, A. Pardo, H. Partridge, T. R. Proctor, K. M. Sando, A. S. Schlachter, W. J. Stevens, D. G. Truhlar, R. Velasco, K. K. Verma, C. R. Vidal , J. K. G. Watson, D. K. Watson, K. R. Way, P. H. Wine, C. Yamada and S. C. Yang.

This work was supported in part by the Critical Compilation Program of the National Bureau of Standards (now the National Institute of Standards and Technology) and by the National Science Foundation.

## 5. Appendix on Isotopic Atomic Energetics

In discussing the isotopomers of lithium hydride, it is useful to also summarize the properties of the fragments of lithium hydride, namely neutral and ionized $^1H$, $^2H$, $^3H$, $^6Li$ and $^7Li$. In particular, the species listed show significant isotope shifts in their excitation and ionization energies; theoretical calculations for these one- (H, $Li^{+2}$), two- ($Li^+$) and three-electron (Li) systems should include reduced mass, relativistic, finite nuclear size and radiative (quantum electrodynamic "Lamb shift") corrections in addition to standard nonrelativistic quantum theory. Fortunately, one- and two-electron atoms and ions are well understood [BET 57] and the three-electron atom Li is pseudohydrogenic. The relative magnitudes of the various ionization potentials and the $D_0^0$ value for the $^n$Li$^m$H species is shown schematically in Fig. 2.

One of the goals of this review is to provide highly accurate descriptions of the isotopic shifts so that one can not only test standard nonrelativistic quantum theories of electron correlation, but also theories of the other smaller corrections.

Let us first consider the one-electron systems $^m$H and $^n$Li$^{+2}$. The fundamental hydrogenic formula is for an infinitely massive, point nucleus and is nonrelativistic. Thus, one must correct [BET 57, JOH 85] for the finite

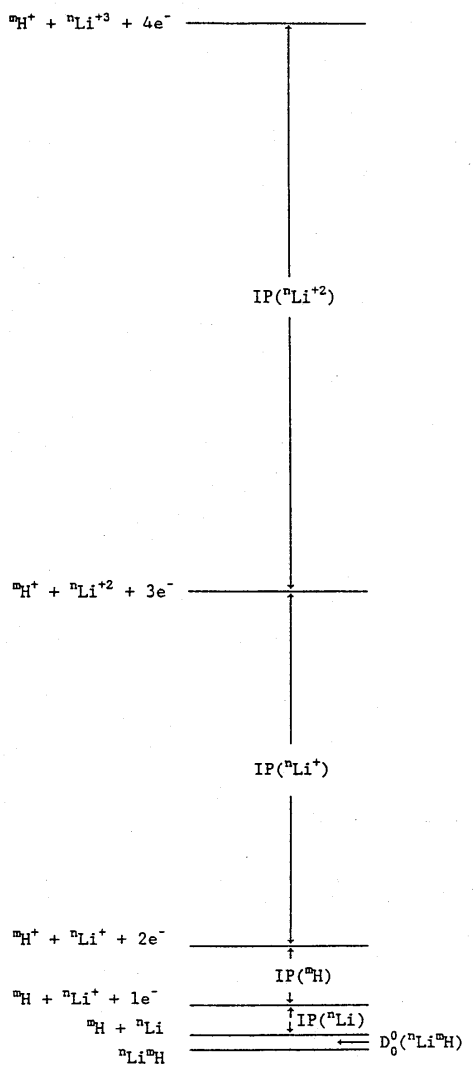


FIG. 2. Schematic diagram of $^n$Li$^m$H energetics.

nuclear mass, the finite size of the nucleus, the effects of relativity, and also the radiative ("Lamb shift") corrections of quantum electrodynamics. It might be noted that, except for the Born-Oppenheimer corrections discussed in Sec. 2.6, all existing *ab initio* calculations of LiH are for infinitely massive, point nuclei and are nonrelativistic.

The energetics of these one-electron species and hypothetical infinite nuclear mass species are given in Tables 18 and 19. The Rydberg constant $R_\infty = 109737.315709(18)$ $cm^{-1}$ is taken from [BIR 89]. The reduced mass values are then computed from the electron, proton and deuteron masses of [COH 87], the triton mass of 3.0155007 amu computed from the tritium mass of [WAP 85], and the nuclear masses of $^6Li^{+3}$ = 6.0134758 amu and of $^7Li^{+3}$ = 7.0143574 amu based on the atomic masses of [WAP 85] and corrected for the total binding energy ($3\times10^{-7}$ amu).

In terms of the quantities defined by [JOH 85], the Dirac Coulomb binding energy of a $1s$ electron in the field of an infinitely massive point nucleus of charge $Z$ is given analytically by the following expression, which includes a relativistic correction:

$$\frac{E^C}{R_\infty} = Z^2\left(1+\frac{1-\sqrt{1-(Z\alpha)^2}}{1+\sqrt{1-(Z\alpha)^2}}\right) = \frac{E^{CN}+\Delta E^{CR}}{R_\infty}$$

where for H, $\Delta E^{CR}/E^{CN}$ = 0.000013313, while for $Li^{+2}$ the ratio is 0.000119844. The reduced mass correction, $\Delta E^{RM}/R_\infty$, can also be divided into the larger nonrelativistic contribution and the much smaller relativistic contribution:

$$\frac{\Delta E^{RM}}{R_\infty} = -Z^2\frac{\mu}{M_N}\left\{1-\left[\frac{(Z\alpha)^2}{4}-\frac{1-\sqrt{1-(Z\alpha)^2}}{1+\sqrt{1+(Z\alpha)^2}}\right.\right.$$

$$\left.\left.+\frac{(Z\alpha)^2}{4}-\frac{1-\sqrt{1-(Z\alpha)^2}}{1+\sqrt{1+(Z\alpha)^2}}\right]\right\} = \frac{\Delta E^{RMN}+\Delta E^{RMR}}{R_\infty}$$

where $\mu = m_e M_N/(m_e+M_N)$ is the reduced mass of the electron and the nucleus ($^mH^+$ or $^nLi^{+3}$), and the term in square brackets gives rise to the $\Delta E^{RMR}$ term. Since the third term in square brackets is 0 ($(Z\alpha)^6$) and the first two terms in the square brackets nearly cancel, the $\Delta E^{RMR}$ term is very small; the brackets factor is $\sim(Z\alpha)^4/8$. For H, $\Delta E^{RMR}/\Delta E^{RMN} = 3.545\times10^{-10}$, while for $Li^{+2}$, the ratio is $2.871\times10^{-8}$, so this relativistic term is negligible. Finally the ratio $\Delta E^{RM}/E^C = -\mu/M_N(1-(Z\alpha)^2/4)$ is −0.000544313, −0.000272366, and −0.000181884 for $^1H$, $^2H$ and $^3H$, respectively, and −0.0000912058 and −0.0000781927 for $^6Li^{+2}$ and $^7Li^{+2}$, respectively.

The smallest term considered by [JOH 85] consists of the "leftovers" and is collectively called the Lamb-shift correction (which we call $\Delta E^Q+\Delta E^{FS}$). For the low $Z$ values (1 and 3) considered here, there are six significant contributions (see Fig. 2 of [JOH 85]):

$$\frac{\Delta E^{LAMB}}{R_\infty} = \frac{1}{R_\infty}\left\{\Delta E^{SELF}+\Delta E^{UEHL}+\Delta E^{HO}+\Delta E^{FS}+\Delta E^{RR}+\Delta E^{RRM}\right\}$$

The first three contributions are radiative (quantum electrodynamic) terms for point nuclei, the fourth contribution arises from the finite size of the nuclei (and is proportional to the square of the nuclear radius), and the last two small relativistic contributions are proportional to the reduced mass. The finite size corrections for $^2H$, $^3H$ and $^6Li$ are estimated from the values for $^1H$ and $^7Li$ using the values of [JOH 85] scaled with the $(r^2)^{1/2}$ values (in $fm$) of 0.850, 2.106, 1.71, 2.55 and 2.392 for $^1H$, $^2H$, $^3H$, $^6Li$ and $^7Li$, respectively [DEV 87].

Note that four levels of approximation are indicated in both tables: *NP* (nonrelativistic, point nucleus); *RP* (relativistic, point nucleus); *QP* (quantum electrodynamic, point nucleus); and *QF* (quantum electrodynamic, finite size nucleus).

For the two-electron systems $^nLi^+$, the most accurate results are theoretical [FRE 84, DRA 88], although the $^7Li^+$ experimental ionization potential with larger uncertainty [CRO 84] is compatible with theory. These results are presented in Table 20, again with total ionization potentials given at four levels of approximation (*NP*, *RP*, *QP* and *QF*).

TABLE 18. Summary of one-electron system energetics (ionization potentials in $cm^{-1}$) for $^mH$

| term | $^\infty H$ | $^1H$ | $^2H$ | $^3H$ |
|---|---|---|---|---|
| $E^{CN}$ (NP) | 109737.315709 | 109677.581430 | 109707.424611 | 109717.353927 |
| $\Delta E^{CR}$ | 1.460933 | 1.460933 | 1.460933 | 1.460933 |
| $E^R$ (RP) | 109738.776642 | 109679.042363 | 109708.885544 | 109718.814860 |
| $\Delta E^Q$ | −0.272933 | −0.270591 | −0.270762 | −0.270819 |
| $E^Q$ (QP) | 109738.503709 | 109678.771772 | 109708.614782 | 109718.544041 |
| $\Delta E^{FS}$ | | −0.000039 | −0.000237 | −0.000156 |
| $E^Q$ (QF) | | 109678.771733 | 109708.614545 | 109718.543885 |

$m_e M_N/(m_e+M_N)$

TABLE 19. Summary of one-electron system energetics (ionization potentials in $cm^{-1}$) for $^nLi^{+2}$

| term | $^\infty Li^{+2}$ | $^6Li^{+2}$ | $^7Li^{+2}$ |
|---|---|---|---|
| $E^{CN}$ (NP) | 987635.8413 | 987545.7980 | 987558.6453 |
| $\Delta E^{CR}$ | 118.3023 | 118.3023 | 118.3023 |
| $E^R$ (RP) | 987754.1496 | 987664.1003 | 987676.9476 |
| $\Delta E^Q$ | −15.9327 | −15.9314 | −15.9316 |
| $E^Q$ (QP) | 987738.2109 | 987648.1689 | 987661.0160 |
| $\Delta E^{FS}$ | | −0.0277 | −0.0244 |
| $E^Q$ (QF) | | 987648.1412 | 987660.9916 |

TABLE 20. Summary of two-electron system energetics (ionization potentials in $cm^{-1}$) for $^{n}Li^{+}$ [DRA 88]

| term | $^{\infty}Li^{+}$ | $^{6}Li^{+}$ | $^{7}Li^{+}$ |
|---|---|---|---|
| $E^{CNa}$ (NP) | 610120.471 | 610059.012 | 610067.776 |
| $\Delta E^{CR}$ | 19.685 | 19.685 | 19.685 |
| $E^{R}$ (RP) | 610140.156 | 610078.697 | 610087.461 |
| $\Delta E^{Q}$ | −8.938 | −8.938 | −8.938 |
| $E^{Q}$ (QP) | 610131.218 | 610069.759 | 610078.523 |
| $\Delta E^{FS}$ | | −0.016 | −0.014 |
| $E^{Q}$ (QF) | | 610069.743 | 610078.509 |

[a] Includes mass polarization (0 for $^{\infty}Li^{+}$, $-5.787\ cm^{-1}$ for $^{6}Li^{+}$ and $-4.960\ cm^{-1}$ for $^{7}Li^{+}$).

Finally, for the three-electron systems $^{n}Li$, theory [MCK 91] and experiment [JOH 59] are in excellent agreement for $^{7}Li$. These results are presented in Table 21, again with ionization potentials given at four levels of approximation (*NP*, *RP*, *QP* and *QF*).

TABLE 21. Summary of three-electron system energetics (ionization potentials in $cm^{-1}$) for $^{n}Li$ [MCK 91]

| term | $^{\infty}Li$ | $^{6}Li$ | $^{7}Li$ |
|---|---|---|---|
| $E^{CNa}$ (NP) | 43488.225 | 43484.003 | 43484.605 |
| $\Delta E^{CR}$ | 2.761 | 2.761 | 2.761 |
| $E^{R}$ (RP) | 43490.986 | 43486.764 | 43487.366 |
| $\Delta E^{Q}$ | −0.215 | −0.215 | −0.215 |
| $E^{Q}$ (QP) | 43490.771 | 43486.549 | 43487.151 |
| $\Delta E^{FS}$ | | 0.000 | 0.000 |
| $E^{Q}$ (QF) | | 43486.549 | 43487.151 |

[a] Includes mass polarization (0 for $^{\infty}Li$, $-0.2561\ cm^{-1}$ for $^{6}Li$ and $-0.2195\ cm^{-1}$ for $^{7}Li$).

The asymptotic energies for the $^{n}Li$ and $^{m}H$ limits with respect to the $^{n}Li^{+3}+{}^{m}H^{+}+4e^{-}$ limits are given in Table 22 in these four approximations. Note that the nonrelativistic, point nuclei approximation for infinitely massive nuclei is most appropriate for comparison with the nonrelativistic, fixed point nuclei, *ab initio* electronic structure calculations of LiH reported above in Table 13. Note also that the relativistic corrections are quite sizable ($\sim 140\ cm^{-1}$), the quantum electrodynamic corrections still significant ($\sim -25\ cm^{-1}$), but the nuclear size corrections very small ($\sim -0.04\ cm^{-1}$). Finally, note that the difference between the asymptote of the lightest isotopomer ($^{6}Li^{1}H$) and the asymptote of the heaviest ($^{7}Li^{3}H$) is only $\sim 60\ cm^{-1}$, but the asymptote of the hypothetical infinitely massive isotopomer $^{\infty}Li^{\infty}H$ is $\sim 200\ cm^{-1}$ greater.

The asymptotic differences in Table 22 correspond to the limiting values of the adiabatic corrections to the Born-Oppenheimer approximation, discussed in Secs. 2.4 and 2.6. For example, for the nonrelativistic, point nucleus values in Table 21, one obtains $\lim_{R\to\infty} \Delta U^{H}(R)$ and $\lim_{R\to\infty} \Delta U^{Li}(R)$ values of $59.528\ cm^{-1}\cdot amu$ and $932.027\ cm^{-1}\cdot amu$, respectively, for the $X\,^{1}\Sigma^{+}$ state of LiH. These values agree well with *ab initio* molecular calculations (at $15\,a_0$ [JEN 88]) of 60.2 and 914.7 $cm^{-1}\cdot amu$, respectively, and values based on atomic calculations [BIS 83] of 60.2 and $936.65\ cm^{-1}\cdot amu$, respectively.

TABLE 22. Energetics ($cm^{-1}$) of the $^{m}H+{}^{n}Li$ asymptotes in various approximations with respect to $^{m}H^{+}+{}^{n}Li^{+3}+4e^{-}$ infinitely separated

| (*m*,*n*) | *NP* | *RP* | *QP* | *QF* |
|---|---|---|---|---|
| 1,6 | 1750766.394 | 1750908.604 | 1750883.249 | 1750883.205 |
| 1,7 | 1750788.608 | 1750930.817 | 1750905.462 | 1750905.423 |
| 2,6 | 1750796.238 | 1750938.447 | 1750913.092 | 1750913.048 |
| 2,7 | 1750818.451 | 1750960.660 | 1750935.305 | 1750935.266 |
| 3,6 | 1750806.167 | 1750948.376 | 1750923.021 | 1750922.977 |
| 3,7 | 1750828.380 | 1750970.590 | 1750945.234 | 1750945.196 |
| 1,∞ | 1750922.119 | 1751064.334 | 1751038.972 | – |
| 2,∞ | 1750951.962 | 1751094.177 | 1751068.815 | – |
| 3,∞ | 1750961.891 | 1751104.107 | 1751078.744 | – |
| ∞,6 | 1750826.129 | 1750966.877 | 1750942.981 | – |
| ∞,7 | 1750848.342 | 1750989.090 | 1750965.194 | – |
| ∞,∞ | 1750981.185 | 1751124.068 | 1751098.704 | – |

## 6. References


ACH 84 Acharya, P. K., R. A. Kendall, and J. Simons, J. Am. Chem. Soc. **106**, 3402 (1984).

ADA 69 Adamov, M. N., N. P. Borisova, and O. Kastano, Teor. Eksp. Khim. **5**, 533 (1969).

ADA 81 Adamowicz, L. and E. A. McCullough, Jr., J. Chem. Phys. **75**, 2475 (1981).

ADA 83 Adamowicz, L. and E. A. McCullough, Jr., Int. J. Quantum Chem. **24**, 19 (1983).

ADA 84 Adamowicz, L. and E. A. McCullough, Jr., J. Phys. Chem. **88**, 2045 (1984).

ADA 85 Adamowicz, L. and R. J. Bartlett, J. Chem. Phys. **83**, 6268 (1985).

ALI 85 Alikacem, A. and M. Aubert-Frecon, J. Mol. Spectrosc. **111**, 20 (1985).

ALL 83 Allan, R. J., A. S. Dickinson, and R. McCarroll, J. Phys. *B* **16**, 467 (1983).

ALV 81 Alvarez, I. T. and C. G. Cisneros, Revista Mexicana de Fisica **27**, 179 (1981).

AND 80 Anderson, C. J., R. J. Girnius, A. M. Howald, and L. W. Anderson, Phys. Rev. A **22**, 822 (1980).

ARR 70 Arrighini, G. P., J. Tomasi, and C. Guidotti, Theoret. Chim. Acta (Berl.) **18**, 329 (1970).

ARR 70A Arrighini, G. P., J. Tomasi, and C. Petrongolo, Theoret. Chim. Acta (Berl.) **18**, 341 (1970).

AUB 75 Aubert, M., N. Bessis, and G. Bessis, Phys. Rev. A **12**, 2298 (1975).

BAL 91 Balková, A., S. A. Kucharski, L. Meissner, and R. J. Bartlett, J. Chem. Phys. **95**, 4311 (1991).

BAR 78 Bardo, R. D., L. I. Kleinman, A. W. Raczkowski, and M. Wolfsberg, J. Chem. Phys. **69**, 1106 (1978).

BAR 87 Barnett, R. N., P. J. Reynolds, and W. A. Lester, Jr., J. Phys. Chem. **91**, 2004 (1987).

BAT 56 Bates, D. R. and T. J. M. Boyd, Proc. Phys. Soc. (London) **69**, 910 (1956).

BEN 66 Bender, C. F. and E. R. Davidson, J. Phys. Chem. **70**, 2675 (1966).

BEN 68 Bender, C. F. and E. R. Davidson, J. Chem. Phys. **49**, 4222 (1968).

BEN 88 Ben-Shlomo, S. and U. Kaldor, J. Chem. Phys. **89**, 956 (1988).

BET 57 Bethe, H. A. and E. E. Salpeter, Quantum Mechanics of One- and Two-Electron Atoms (Academic, New York, 1957).

BIR 89 Biraben, F., J. C. Garreau, L. Julien, and M. Allegrini, Phys. Rev. Lett. **62**, 621 (1989).

BIS 83 Bishop, D. M. and L. M. Cheung, J. Chem. Phys. **78**, 1396 (1983).

BIS 83A Bishop, D. M. and L. M. Cheung, J. Chem. Phys. **79**, 2945 (1983).

BIS 83B Bishop, D. M. and L. M. Cheung, J. Chem. Phys. **79**, 7265 (1983).

BIS 85 Bishop, D. M. and B. Lam, Chem. Phys. Lett. **120**, 69 (1985).

BLU 74 Blustin, P. H. and J. W. Linnett, J. Chem. Soc. Faraday Trans. II **70**, 327 (1974).

BRA 82 Bransden, B. H. and C. J. Noble, J. Phys. *B* **15**, 451 (1982).

BRI 80 Brieger, M., A. Hese, A. Renn, and A. Sodeik, Chem. Phys. Lett. **76**, 465 (1980).

BRI 83 Brieger, M., A. Renn, A. Sodeik, and A. Hese, Chem. Phys. **75**, 1 (1983).

BRI 84 Brieger, M., Chem. Phys. **89**, 275 (1984).

BRO 64 Browne, J. C., J. Chem. Phys. **41**, 3495 (1964).

BRO 68 Brown, R. E. and H. Shull, Int. J. Quantum Chem. **2**, 663 (1968).

BUN 77 Bunker, P. R., J. Mol. Spectrosc. **68**, 367 (1977).

BUS 86 Bussery, B., M. Aubert-Frecon, and M. Saute, Chem. Phys. **109**, 39 (1986).

CAD 67 Cade, P. E. and W. M. Huo, J. Chem. Phys. **47**, 614 (1967).

CAR 86 Cardelino, B. H., W. H. Eberhardt, and R. F. Borkman, J. Chem. Phys. **84**, 3230 (1986).

CAS 64 Cashion, J. K., J. Chem. Phys. **41**, 3988 (1964).

CAS 84 Casaubon, J. I. and R. D. Piacentini, J. Phys. *B* **17**, 1623 (1984).

CHA 83 Chan, Y. C. and W. C. Stwalley, J. Chem. Thermodynamics **15**, 995 (1983).

CHA 86 Chan, Y. C., D. R. Harding, W. C. Stwalley, and C. R. Vidal, J. Chem. Phys. **85**, 2436 (1986).

CHO 91 Chong, K. T., Phys. Rev. A **44**, 5421 (1991).

CIM 80 Cimiraglia, R., M. Persico, and J. Tomasi, Chem. Phys. **53**, 357 (1980).

CLA 70 Claxton, T. A. and D. M. McWilliams, J. Chem. Soc. Faraday Trans. II **66**, 573 (1970).

CLA 77 Clary, D. C. and N. C. Handy, Chem. Phys. Lett. **51**, 483 (1977).

COH 87 Cohen, E. R. and B. N. Taylor, Rev. Mod. Phys. **59**, 1121 (1987).

COH 90 Cohen, E. R. and B. N. Taylor, Phys. Today **43**, 9 (1990).

COL 74 Colbourn, E. A. and C. A. Coulson, J. Phys. *B* **7**, 1574 (1974).

COL 80 Collins, L. A., W. D. Robb, and M. A. Morrison, Phys. Rev. A **21**, 488 (1980).

COL 85 Cole, H. R. and R. E. Olson, Phys. Rev. A **31**, 2137 (1985).

COO 85 Cooper, D. L., J. Gerratt, and M. Raimondi, Chem. Phys. Lett. **118**, 580 (1985).

COO 91 Cooper, D. L., J. Gerratt, and M. Raimondi, Chem. Rev. **91**, 929 (1991).

COX86 Coxon, J. A., J.Mol. Spectrosc. **117**, 361 (1986).

COX92 Coxon, J. A., J.Mol. Spectrosc. **152**, 274 (1992).

CRA 35 Crawford, F. H. and T. Jorgensen, Jr., Phys. Rev. **47**, 358 (1935).

CRA 35A Crawford, F. H. and T. Jorgensen, Jr., Phys. Rev. **47**, 932 (1935).

CRA 36 Crawford, F. H. and T. Jorgensen, Jr., Phys. Rev. **49**, 745 (1936).

CRO 84 Crossley, R., J. Opt. Soc. Am. *B* **1**, 266 (1984).

CSI 66 Csizmadia, I. G., J. Chem. Phys. **44**, 1849 (1966).

DAB 81 Daborn, G. T. and N. C. Handy, Chem. Phys. Lett. **81**, 201 (1981).

DAG 76 Dagdigian, P. J., J. Chem. Phys. **64**, 2609 (1976).

DAG 80 Dagdigian, P. J., Chem. Phys. **52**, 279 (1980).

DAG 80A Dagdigian, P. J., in Electronic and Atomic Collisions, edited by N. Oda and K. Takayanagi (North-Holland Publishing Company, Amsterdam, 1980), p. 513.

DAG 80B Dagdigian, P. J., J. Chem. Phys. **73**, 2049 (1980).

DAG 83 Dagdigian, P. J., in Energy Storage and Redistribution in Molecules, edited by J. Hinze (Plenum Press, New York, 1983), p. 149.

DAL 59 Dalgarno, A. and A. E. Kingston, Proc. Phys. Soc. (London) **73**, 455 (1959).

DAL 66 Dalgarno, A. and W. D. Davison, Advan. At. Mol. Phys. **2**, 1 (1966).

DEL 64 De La Vega, J. R., and H. F. Hameka, J. Chem. Phys. **40**, 1929 (1964).

DEV 87 DeVries, H., C. W. DeJager, and C. DeVries, Atomic Data and Nuclear Data Tables **36**, 495 (1987).

DIX 88 Dixon, D. A., J. L. Gole, and A. Komornicki, J. Phys. Chem. **92**, 2134 (1988).

DOC 72 Docken, K. K. and J. Hinze, J. Chem. Phys. **57**, 4928 (1972).

DOC 72A Docken, K. K. and J. Hinze, J. Chem. Phys. **57**, 4936 (1972).

DOC 74 Docken, K. K. and R. R. Freeman, J. Chem. Phys. **61**, 4217 (1974).

DOC 75 Docken, K. K., Chem. Phys. Lett. **30**, 334 (1975).

DOD 77 Dodds, J. L., R. McWeeny, and A. J. Sadlej, Molec. Phys. **34**, 1779 (1977).

DRA 88 Drake, G. W., Can. J. Phys. **66**, 586 (1988).

DUN 32 Dunham, J. L., Phys. Rev. 41, **713** (1932).

DYA 68 D'yachkov, B. A. and V. I. Zinenko, Atomnaya Energiya **24**, 18 (1968).

DYA 69 D'yachkov, B. A., Sov. Phys.-Tech. Phys. **13**, 1036 (1969).

DYA 72 D'yachkov, B. A., V. I. Zinenko, and M. A. Pavlii, Sov. Phys.-Tech. Phys. **16**, 1868 (1972).

DYE 86 Dyer, S. and E. Steiner, Mol. Phys. **59**, 1027 (1986).

ENN 75 Ennen, G. and Ch. Ottinger, Chem. Phys. Lett. **36**, 16 (1975).

ENN 81 Ennen, G., B. Fiedler, and Ch. Ottinger, J. Chem. Phys. **75**, 59 (1981).

ERM 84 Ermolaev, A. M., J. Phys. B **17**, 1069 (1984).

ERR 84 Errea, L. F., L. Mendez, and A. Riera, Chem. Phys. Lett. **104**, 401 (1984).

ERR 85 Errea, L. F., L. Mendez, A. Riera, M. Yanez, J. Hanssen, C. Harel, and A. Salin, J. Physique **46**, 709 (1985).

ERR 85A Errea, L. F., L. Mendez, A. Riera, M. Yanez, J. Hanssen, C. Harel, and A. Salin, J. Physique **46**, 719 (1985).

FAL 60 Fallon, R. J., J. T. Vanderslice, and E. A. Mason, J. Chem. Phys. 33, 944 (1960); J. Chem. Phys. **32**, 1453 (1960).

FER 69 Fernandez-Florez, I. and R. Velasco, Optica Pura y Aplicada **2**, 123 (1969).

FIG 85 Figari, G., G. F. Musso, and V. Magnasco, Molec. Phys. **54**, 689 (1985).

FOR 89 Ford, M. J., D. L. Cooper, J. Gerratt, and M. Raimondi, J. Chem. Soc., Faraday Trans. 2 **85**, 1713 (1989).

FRA 61 Fraga, S. and B. J. Ransil, J. Chem. Phys. **35**, 669 (1961).

FRE 75 Freeman, R. R., A. R. Jacobson, D. W. Johnson, and N. F. Ramsey, J. Chem. Phys. **63**, 2597 (1975).

FRE 84 Freund, D. E., B. D. Huxtable, and J. D. Morgan, Phys. Rev. A **29**, 980 (1984).

FRI 83 Fritsch, W. and C. D. Lin, J. Phys. B **16**, 1595 (1983).

FRO 67 Frost, A. A., J. Chem. Phys. **47**, 3707 (1967).

FUE 82 Fuentealba, P., H. Preuss, H. Stoll, and L. Von Szentpaly, Chem. Phys. Lett. **89**, 418 (1982).

FUE 87 Fuentealba, P., O. Reyes, H. Stoll, and H. Pruess, J. Chem. Phys. **87**, 5338 (1987).

GAR 79 Garrett, W. R., J. Chem. Phys. **71**, 651 (1979).

GAR 82 Garrett, W. R., J. Chem. Phys. **77**, 3666 (1982).

GAT 80 Gatti, C., S. Polezzo, M. Raimondi and M. Simonetta, Molec. Phys. **41**, 1259 (1980).

GAY 68 Gaydon, A. G., Dissociation Energies and Spectra of Diatomic Molecules, 3rd Edition (Chapman and Hall Ltd., London, 1968).

GHO 81 Ghodgaonkar, A. M. and K. Ramani, J. Chem. Soc., Faraday Trans. 2 **77**, 209 (1981).

GIE 91 Gieler, M., F. Aumayr, P. Ziegelwanger, H. Winter, and W. Fritsch, Phys. Rev. A **43**, 127 (1991).

GRA 92 Grabandt, O., H. J. Bakker, and C. A. de Lange, Chem. Phys. Lett. **189**, 291 (1992).

GRI 74 Grice, R. and D. R. Herschbach, Molec. Phys. **27**, 159 (1974).

GRI 75 Griffing, K. M., J. Kenney, J. Simons, and K. D. Jordan, J. Chem. Phys. **63**, 4073 (1975).

GRU 69 Gruebler, W., P. A. Schmelzbach, V. Koenig, and P. Marmier, Phys. Lett. A **29**, 440 (1969).

GRU 70 Gruebler, W., P. A. Schmelzbach, V. Koenig, and P. Marmier, Helvetica Physica Acta **43**, 254 (1970).

GUO 87 Guo, K., W. L. Jarrett, and L. G. Butler, Inorg. Chem. **26**, 3001 (1987).

HAD 86 Hadinger, G. and Y. S. Tergiman, J. Chem. Phys. **85**, 6853 (1986).

HAL 67 Halmann, M. and I. Laulicht, J. Chem. Phys. **46**, 2684 (1967).

HAL 77 Haley, L. V. and H. F. Hameka, Int. J. Quantum Chem. **11**, 733 (1977).

HAN 84 Handy, N. C., R. J. Harrison, P. J. Knowles, and H. F. Schaefer III, J. Phys. Chem. **88**, 4852 (1984).

HER 50 Herzberg, G., Spectra of Diatomic Molecules, 2nd Edition, (Van Nostrand-Reinhold, New York, 1950).

HIR 92 Hirota, E., Chem. Rev. **92**, 141 (1992).

HO 85 Ho, T. S., C. Laughlin, and S. I. Chu, Phys. Rev. A **32**, 122 (1985).

HOE 80 Hoeller, R. and H. Lischka, Molec. Phys. **41**, 1017 (1980).

HOT 85 Hotop, H. and W. C. Lineberger, J. Phys. Chem. Ref. Data **14**, 731 (1985).

HOU 80 Hout, R. F. Jr., M. Wolfsberg, and W. J. Hehre, J. Am. Chem. Soc. **102**, 3296 (1980).

HUB 85 Huber, H., J. Mol. Struct. **121**, 207 (1985).

IBB 81 Ibbs, K. G., P. H. Wine, K. J. Chung, and L. A. Melton, J. Chem. Phys. **74**, 6212 (1981).

IHL 75 Ihle, H. R. and C. H. Wu, J. Chem. Phys. **63**, 1605 (1975).

ILI 67 Il'in, R. N., V. A. Oparin, E. S. Solov'ev, and N. V. Fedorenko, Sov. Phys.-Tech. Phys. **11**, 921 (1967).

JAM 60 James, T. C., W. G. Norris, and W. Klemperer, J. Chem. Phys. **32**, 728 (1960).

JAN 76 Janev, R. K., J. Chem. Phys. **64**, 1891 (1976).

JAN 78 Janev, R. K. and Z. M. Radulovic, Phys. Rev. A **17**, 889 (1978).

JEN 66 Jenč,F., J. Mol. Spectrosc. **19**, 63 (1966).

JEN 85 Jenč,F. and B. A. Brandt, J. Chem. Phys. **83**, 5486 (1985).

JEN 86 Jenč,F. and B. A. Brandt, J. Chem. Phys. **85**, 3702 (1986).

JEN 88 Jensen, J. O. and D. R. Yarkony, J. Chem. Phys. **89**, 975 (1988).

JEN 91 Jenč,F. and B. A. Brandt, Spectrochimica Acta **47A**, 141 (1991).

JOE 81 Joensson, B., B. O. Roos, P. R. Taylor, and Per E. M. Siegbahn, J. Chem. Phys. **74**, 4566 (1981).

JOH 59 Johansson, I., Arkiv foer Fysik **15**, 169 (1959).

JOH 85 Johnson, W. R. and G. Soff, Atomic Data and Nuclear Data Tables **33**, 405 (1985).

JOR 76 Jordan, K. D., K. M. Griffing, J. Kenney, E. L. Andersen, and J. Simons, J. Chem. Phys. **64**, 4730 (1976).

JOR 78 Jordan, K. D. and J. J. Wendoloski, Molec. Phys. **35**, 223 (1978).

JOU 88 Joulakian, B., Chem. Phys. Lett. **143**, 445 (1988).

KAR 59 Karo, A. M. and A. R. Olson, J. Chem. Phys. **30**, 1232 (1959).

KAR 59A Karo, A. M. J. Chem. Phys. **30**, 1241 (1959).

KAR 60 Karo, A. M. J. Chem. Phys. **32**, 907 (1960).

KAR 63 Karplus, M. and H. J. Kolker, J. Chem. Phys. **38**, 1263 (1963).

KAR 78 Karo, A. M., M. A. Gardner, and J. R. Hiskes, J. Chem. Phys. **68**, 1942 (1978).

KAU 83 Kaur, A. J., P. C. Jain, P. S. Bakhshi, and J. Shanker, Indian J. Chem. **22A**, 595 (1983).

KEI 79 Keil, F. and R. Ahlrichs, J. Chem. Phys. **71**, 2671 (1979).

KIM 82 Kimura, M., R. E. Olson, and J. Pascale, Phys. Rev. A **26**, 3113 (1982).

KIR 78 Kirby, K. and A. Dalgarno, Astrophys. J. **224**, 444 (1978).

KLE 55 Klemperer, W., J. Chem. Phys. **23**, 2452 (1955).

KLE 73 Kleinman, L. I. and M. Wolfsberg, J. Chem. Phys. **59**, 2043 (1973).

KLE 74 Kleinman, L. I. and M. Wolfsberg, J. Chem. Phys. **60**, 4740 (1974).

KLE 74A Kleinman, L. I. and M. Wolfsberg, J. Chem. Phys. **60**, 4749 (1974).

KLI 80 Klimo, V. and J. Tino, Molec. Phys. **41**, 483 (1980).

KNO 69 Knox, H. O. and M. R. H. Rudge, Molec. Phys. **17**, 377 (1969).

KOS 74 Kosman, W. M. and J. Hinze, J. Mol. Spectrosc. **51**, 341 (1974).

KOU 73 Kouba, J. E. and W. J. Meath, Mol. Phys. **26**, 1397 (1973).

KOU 74 Kouba, J. E. and W. J. Meath, Mol. Phys. **28**, 829 (1974).

KRA 67 Krauss, M., NBS Tech. Note 438 (Dept. of Commerce, 1967).

KRA 70 Kramer, H., J. Chem. Phys. **53**, 2783 (1970).

KRU 63 Krupenie, P. H., E. A. Mason, and J. T. Vanderslice, J. Chem. Phys. **39**, 2399 (1963).

KUB 81 Kubach, C. and V. Sidis, Phys. Rev. A **23**, 110 (1981).

KUL 79 Kulkarni, S. V. and L. K. Sharma, Indian J. Phys. A **53**, 616 (1979).

KUM 86 Kumar, M., A. J. Kaur, and J. Shanker, J. Chem. Phys. **84**, 5735 (1986).

KUP 74 Kuprievich, V. A., O. V. Shramko, and V. E. Krimenko, Theor. and Experimental Chem. (Russian) **10**, 746 (1974).

KUR 85 Kurtz, H. A., B. Weiner, and Y. Ohrn, in Comparison of Ab Initio Quantum Chemistry with Experiment for Small Molecules, edited by R. Bartlett, (D. Reidel, New York, 1985), p. 339.

LAN 78 Langhoff, S. R. and D. P. Chong, J. Chem. Phys. **69**, 194 (1978).

LAW 63 Lawrence, T. R., C. H. Anderson, and N. F. Ramsey, Phys. Rev. **130**, 1865 (1963).

LAZ 82 Lazzeretti, P., E. Rossi and R. Zanasi, J. Phys. B **15**, 521 (1982).

LER 70 LeRoy, R. J., J. Chem. Phys. **52**, 2683 (1970).

LES 90 Lester, W. A. Jr. and B. L. Hammond, Annu. Rev. Phys. Chem. **41**, 283 (1990).

LI 78 Li, K. C. and W. C. Stwalley, J. Mol. Spectrosc. **69**, 294 (1978).

LI 79 Li, K. C. and W. C. Stwalley, J. Chem. Phys. **70**, 1736 (1979).

LIN 69 Lin, C. S., J. Chem. **50**, 2787 (1969).

LIU 77 Liu, B., K. O-Ohata, and K. Kirby-Docken, J. Chem. Phys. **67**, 1850 (1977).

LOD 69 Lodge, J. G., J. Phys. B **2**, 322 (1969).

LUH 88 Luh, W. T., P. D. Kleiber, A. M. Lyyra, and W. C. Stwalley, J. Mol. Spectrosc. **129**, 388 (1988).

MAK 90 Maki, A. G., W. B. Olson, and G. Thompson, J. Mol. Spectrosc. **144**, 257 (1990).

MAL 85 Malik, D. J. and C. E. Dykstra, J. Chem. Phys. **83**, 6307 (1985).

MAN 81 Mandal, C. R., S. Datta, and S. C. Mukherjee, Phys. Rev. A **24**, 3044 (1981).

MAR 86 Maroulis, G. and D. M. Bishop, Theor. Chim. Acta **69**, 161 (1986).

MCC 81 McCullough, Jr., E. A., J. Chem. Phys. **75**, 1579 (1981).

MCK 91 McKenzie, D. K. and G. W. F. Drake, Phys. Rev. A **44**, R6973 (1991).

MEL 72 Melius, C. F. and W. A. Goddard III, J. Chem. Phys. **56**, 3348(1972).

MEL 77 Melton, L. A. and P. H. Wine, ACS Symposium Ser., **56**, 167 (1977).

MEN 90 Mendez, L., I. L. Cooper, A. S. Dickinson, O. Mo and A. Riera, J. Phys. B **23**, 2797 (1990).

MEY 75 Meyer, W. and P. Rosmus, J. Chem. Phys. **63**, 2356 (1975).

MOO 71 Moore, C. E., Atomic Energy Levels, Vol I-III, NSRDS-NBS 35 (U. S. Government Printing Office, Washington, DC 1971).

MOR 85 Morgan, T. J., R. E. Olson, A. S. Schlachter, and J. W. Gallagher, J. Phys. Chem. Ref. Data **14**, 971 (1985).

MUK 70 Mukherjee, N. G. and R. McWeeny, Int. J. Quantum Chem. **4**, 97 (1970).

MUL 36 Mulliken, R. S., Phys. Rev. **50**, 1028 (1936).

NAK 30 Nakamura, G., Z. Phys. **59**, 218 (1930).

NAK 31 Nakamura, G. and T. Shidei, Jpn. J. Phys. **7**, 33 (1931).

NAZ 89 Nazarenko, T. G., Opt. Spectrosc. (USSR) **66**, 326 (1989).

NOR 58 Norris, W. G. and W. Klemperer, J. Chem. Phys. **28**, 749 (1958).

OGI 87 Ogilvie, J. F., Chem. Phys. Lett. **140**, 506 (1987).

OGI 90 Ogilvie, J. F., Spectrochimica Acta **46A**, 43 (1990).

OGI 91 Ogilvie, J. F., J. Mol. Spectrosc. **148**, 243 (1991); see [COX 92] also.

OLS 71 Olson, R. E., F. T. Smith, and E. Bauer, Appl. Opt. **10**, 1848 (1971).

OLS 82 Olson, R. E., J. Phys. B **15**, L163 (1982).

OPP 74 Oppenheimer, M. and K. K. Docken, Chem. Phys. Lett. **29**, 349 (1974).

ORT 79 Orth, F. B. and W. C. Stwalley, J. Mol. Spectrosc. **76**, 17 (1979).

PAI 90 Paidarova, I., J. Vojtik, L. Cespiva, J. Savrda, and V. Spirko, Int. J. Quantum Chem. **38**, 283 (1990).

PAL 69 Palke, W. E. and W. A. Goddard III, J. Chem. Phys. **50**, 4524 (1969).

PAR 81 Partridge, H. and S. R. Langhoff, J. Chem. Phys. **74**, 2361 (1981).

PAR 81A Partridge, H., S. R. Langhoff, W. C. Stwalley, and W. T. Zemke, J. Chem. Phys. **75**, 2299 (1981).

PAR 86 Pardo, A., J. Mol. Struct. **141**, 137 (1986).

PAR 86A Pardo, A., J. J. Camacho, and J. M. L. Poyato, Chem. Phys. Lett. **131**, 490 (1986).

PAR 86B Pardo, A., J. J. Camacho, and J. M. L. Poyato, Chem. Phys. **108**, 15 (1986).

PAR 88 Pardo, A., J. J. Camacho, J. M. L. Poyato, E. Martin, and D. Reyman, J. Mol. Struct. **166**, 181 (1988).

PEA 69 Pearson, E. F. and W. Gordy, Phys. Rev. **177**, 59 (1969).

PEA 84 Pearson, E. W., M. D. Jackson, and R. G. Gordon, J. Phys. Chem. **88**, 119 (1984).

PEA 89 Peacher, J. L., E. Redd, D. G. Seely, T. J. Gay, D. M. Blankenship, and J. T. Park, Phys. Rev. A **39**, 1760 (1989).

PIE 84 Pietrovito, A. J., H. F. Hameka, and D. Zeroka, J. Chem. Phys. **81**, 1960 (1984).

PLA 59 Platas, O., R. P. Hurst, and F. A. Matsen, J. Chem. Phys. **31**, 501 (1959).

PLU 84 Plummer, G. M., E. Herbst, and F. C. De Lucia, J. Chem. Phys. **81**, 4893 (1984).

PRA 79 Prasad, S. C., N. N. Singh, and K. P. Thakurr, J. Chem. Soc., Faraday Trans. 2 **75**, 1717 (1979).

PRO 77 Proctor, T. R. and W. C. Stwalley, J. Chem. Phys. **66**, 2063 (1977).

RAF 83 Rafi, M., Z. Iqbal, and M. A. Baig, Z. Phys. A **312**, 357 (1983).

RAY 79 Ray, N. K., L. Samuels, and R. G. Parr, J. Chem. Phys. **70**, 3680 (1979).

REI 86 Reinhold, C. O. and C. A. Falcon, Phys. Rev. A **33**, 3859 (1986).

REQ 87 Requena, A., J. Zuniga, and Y. A. Hidalgo, Anales Quimica **83A**, 343 (1987).

RER 91 Rerat, M., C. Pouchan, M. Tedjeddine, J. P. Flament, H. P. Gervais and G. Berthier, Phys. Rev. A **43**, 5832 (1991).

REY 82 Reynolds, P. J., D. M. Ceperley, B. J. Alder, and W. A. Lester, J. Chem. Phys. **77**, 5593 (1982).

RIC 71 Richards, W. G., T. E. H. Walker, and R. K. Hinkley, Bibliography of Ab Initio Molecular Wave Functions (Oxford University Press, Oxford, 1971).

RIC 74 Richards, W. G., T. E. H. Walker, L. Aarnell, and P. R. Scott, Bibliography of Ab Initio Molecular Wave Functions: Supplement for 1970–1973 (Oxford University Press, Oxford, 1974).

RIC 78 Richards, W. G., P. R. Scott, E. A. Colbourn, and A. F. Marchington, Bibliography of Ab Initio Molecular Wave Functions: Supplement for 1974–1977 (Oxford University Press, Oxford, 1978).

RIC 81 Richards, W. G., P. R. Scott, V. Seckwild, and S. A. Robins, Bibliography of Ab Initio Molecular Wave Functions: Supplement for 1978–1980 (Oxford University Press, Oxford, 1981).

ROO 82 Roos, B. O. and A. J. Sadlej, J. Chem. Phys. **76**, 5444 (1982).

ROO 85 Roos, B. O. and A. J. Sadlej, Chem. Phys. **94**, 43 (1985).

ROS 77 Rosmus, P. and W. Meyer, J. Chem. Phys. **66**, 13 (1977).

ROS 78 Rosmus, P. and W. Meyer, J. Chem. Phys. **69**, 2745 (1978).

ROT 69 Rothstein, E., J. Chem. Phys. **50**, 1899 (1969).

SAH 69 Sahni, R. C., B. C. Sawhney and M. J. Hanley, J. Chem. Phys. **51**, 539 (1969).

SAN 38 Sandeman, I., Proc. Royal Soc. Edinburgh **59**, 1 (1938–39).

SAN 39 Sandeman, I., Proc. Royal Soc. Edinburgh **59**, 130 (1939).

SAN 40 Sandeman, I., Proc. Royal Soc. Edinburgh **60**, Pt. 2, 210 (1939–40).

SAS 90 Sasagane, K., K. Mori, A. Ichihara, and R. Itoh, J. Chem. Phys. **92**, 3619 (1990).

SAT 83 Sato, H. and M. Kimura, Phys. Lett. A **96**, 286 (1983).

SCH 72 Schwartz, M. E., and J. D. Switalski, J. Chem. Phys. **57**, 4132 (1972).

SEL 75 Selsby, R. G., Int. J. Quantum Chem. **9**, 83 (1975).

SEW 80 Sewell, E. C., G. C. Angel, K. F. Dunn, and H. B. Gilbody, J. Phys. B **13**, 2269 (1980).

SHA 91 Shah, M. B. and H. B. Gilbody, J. Phys. B **24**, 977 (1991).

SHP 79 Shpil'rain, E. E. and A. Ya. Polishchuk, Teplofizika Vysokikh Temperatur **17**, 285 (1979).

SIN 62 Singh, N. L. and D. C. Jain, Proc. Phys. Soc. **79**, 274 (1962).

SIN 62A Singh, N. L. and D. C. Jain, Proc. Phys. Soc. **79**, 753 (1962).

STA 68 Stacey, G. W. and A. Dalgarno, J. Chem. Phys. **48**, 4512 (1968).

STE 40 Stevenson, D. P., J. Chem. Phys. **8**, 898 (1940).

STE 63 Stevens, R. M., R. M. Pitzer, and W. N. Lipscomb, J. Chem. Phys. **38**, 550 (1963).

STE 75 Stewart, R. F., D. K. Watson, and A. Dalgarno, J. Chem. Phys. **63**, 3222 (1975).

STE 81 Stevens, W. J., A. M. Karo, and J. R. Hiskes, J. Chem. Phys. **74**, 3989 (1981).

STW 74 Stwalley, W. C., K. R. Way, and R. Velasco, J. Chem. Phys. **60**, 3611 (1974).

STW 75 Stwalley, W. C., J. Chem. Phys. **63**, 3062 (1975).

STW 77 Stwalley, W. C., W. T. Zemke, K. R. Way, K. C. Li, and T. R. Proctor, J. Chem. Phys. **66**, 5412 (1977); J. Chem. Phys. **67**, 4785 (1977).

STW 82 Stwalley, W. C., K. K. Verma, A. Rajaei-Rizi, J. T. Bahns, and D. R. Harding, Proceedings of the Lasers '81 Conf., p. 205 (1982).

STW 91 Stwalley, W. C., W. T. Zemke, and S. C. Yang, J. Phys. Chem. Ref. Data **20**, 153 (1991).

SUN 84 Sundholm, D., P. Pyykkoe, L. Laaksonen, and A. J. Sadlej, Chem. Phys. Lett. **112**, 1 (1984).

SUN 85 Sundholm, D., P. Pyykkoe, and L. Laaksonen, Mol. Phys. **55**, 627 (1985).

SUN 88 Sundholm, D., Chem. Phys. Lett. **149**, 251 (1988).

TAN 76 Tang, K. T., J. M. Norbeck, and P. R. Certain, J. Chem. Phys. **64**, 3063 (1976).

TAY 63 Taylor, H. S., J. Chem. Phys. **39**, 3382 (1963).

TIL 91 Till, S. J., S. T. Howard, and I. W. Parsons, J. Chem. Phys. **95**, 9079 (1991).

TOR 78 Tortorelli, J. J. and J. E. Harriman, J. Chem. Phys. **69**, 3163 (1978).

URB 90 Urban, M. and A. J. Sadlej, Chem. Phys. Lett. **173**, 157 (1990).

VAR 63 Varshni, Y. P. and R. C. Shukla, Rev. Mod. Phys. **35**, 130 (1963).

VAR 84 Varghese, S. L., W. Waggoner, and C. L. Cocke, Phys. Rev. A **29**, 2453 (1984).

VAR 88 Varshni, Y. P., Can. J. Chem. **66**, 763 (1988).

VEL 57 Velasco, R., Can. J. Phys. **35**, 1204 (1957).

VEL 74 Velasco, R., Optica Pura y Aplicada **7**, 14 (1974).

VEL 74A Velasco, R. and F. Rivero, Optica Pura y Aplicada **7**, 45 (1974).

VER 82 Verma, K. K. and W. C. Stwalley, J. Chem. Phys. **77**, 2350 (1982).

VID 77 Vidal, C. R. and H. Scheingraber, J. Mol. Spectrosc. **65**, 46 (1977).

VID 82 Vidal, C. R. and W. C. Stwalley, J. Chem. Phys. **77**, 883 (1982).

VID 84 Vidal, C. R. and W. C. Stwalley, J. Chem. Phys. **80**, 2697 (1984).

VOJ 85 Vojtik, J., V. Riha, and J. Savrda, Chem. Phys. Lett. **115**, 549(1985).

VOJ 90 Vojtik, J., L. Cespiva, J. Savrda, and I. Paidarova, J. Mol. Spectrosc. **142**, 279 (1990).

VON 87 Von Moers, F., S. Heitz, H. Buesener, H. J. Sagner, and A. Hese, Chem. Phys. **116**, 215 (1987).

WAN 89 Wang, X. C. and K. F. Freed, J. Chem. Phys. **91**, 3002 (1989).

WAP 77 Wapstra, A. H. and K. Bos, At. Data Nucl. Data Tables **19**, 177 (1977).

WAP 85 Wapstra, A. H. and G. Audi, Nucl. Phys. A **432**, 1 (1985).

WAT 73 Watson, J. K. G., J. Mol. Spectrosc. **45**, 99 (1973).

WAT 76 Watson, D. K., R. F. Stewart, and A. Dalgarno, Molec. Phys. **32**, 1661 (1976).

WAT 80 Watson, J. K. G., J. Mol. Spectrosc. **80**, 411 (1980).

WAY 73 Way, K. R. and W. C. Stwalley, J. Chem. Phys. **59**, 5298 (1973).

WEI 87 Weiner, B. and Y. Ohrn, J. Phys. Chem. **91**, 563 (1987).

WHA 60 Wharton, L., L. P. Gold, and W. Klemperer, J. Chem. Phys. **33**, 1255 (1960).

WHA 62 Wharton, L., L. P. Gold, and W. Klemperer, J. Chem. Phys. **37**, 2149 (1962).

WHA 92 Whang, T. J., W. T. Zemke, and W. C. Stwalley, to be submitted.

WIL 82 Wilson, S. and D. M. Silver, J. Chem. Phys. **77**, 3674 (1982).

WIN 76 Wine, P. H. and L. A. Melton, J. Chem. Phys. **64**, 2692 (1976).

YAM 88 Yamada, C. and E. Hirota, J. Chem. Phys. **88**, 6702 (1988).

YAN 82 Yang, S. C. and W. C. Stwalley, ACS Symp. Series **179**, 241 (1982).

YAR 76 Yardley, R. N. and G. G. Balint-Kurti, Molec. Phys. **31**, 921 (1976).

ZEM 78 Zemke, W. T. and W. C. Stwalley, J. Chem. Phys. **68**, 4619 (1978).

ZEM 78A Zemke, W. T., J. B. Crooks, and W. C. Stwalley, J. Chem. Phys. **68**, 4628 (1978).

ZEM 78B Zemke, W. T., K. R. Way, and W. C. Stwalley, J. Chem. Phys. **69**, 402 (1978).

ZEM 78C Zemke, W. T. and W. C. Stwalley, J. Chem. Phys. **69**, 409 (1978).

ZEM 79 Zemke, W. T., K. M. Sando, and W. C. Stwalley, unpublished results; preliminary results were first given at the 34th Symposium on Molecular Spectroscopy (Columbus, OH, June 1979).

ZEM 80 Zemke, W. T. and W. C. Stwalley, J. Chem. Phys. **73**, 5584 (1980).

ZEM 81 Zemke, W. T., K. K. Verma, and W. C. Stwalley, Proc. Int. Conf. Lasers '81, December 14–18, 1981, p. 216.